HGF stimulation. Moreover, a combined treatment with TGF-β and HGF of the cells expressing Smad3(3S-A) led to an additional increase in the activity. These results were similar to those in cotransfection with Smad3WT.

We further investigated effects of Smad3 phosphorylation on another transcriptional activity. For the assays, we used $(SBE)_4$-Luc, because TGF-β-induced activation of $(SBE)_4$-Luc, driven by four repeats of the CAGACA sequence identified as Smad binding element in the *JunB* promoter (Jonk *et al*., 1998), was dependent on expression of Smad3, but not on expression of Smad2 (Piek *et al*., 2001). Treatment with either TGF-β or HGF induced an increase in $(SBE)_4$-luciferase reporter activation (Figure 8d). Moreover, additional treatment of HGF with TGF-β led to an increase in the transcriptional activity. HGF treatment of the cells expressing either Smad3WT or Smad3(3S-A) led to increase in the activity. However, cotransfection with Smad3EPSM could not lead to an activation of the $(SBE)_4$-luciferase reporter in RGM-1 cells treated with HGF. Collectively, HGF signaling pathway alone increases transcriptional activities of PF1-Luc and $(SBE)_4$-Luc in RGM-1 cells. In addition, it enhances TGF-β signal through Smad3 phosphorylation at the linker region.

Activation of $p15^{INK4B}$ promoter requires not linker but C-terminal phosphorylation of Smad3

In most epithelial cells, signaling mediated by receptor tyrosine kinases antagonized the antiproliferative effect of TGF-β (Roberts *et al*., 1985). In this respect, we also observed that the antiproliferative effect of TGF-β on RGM-1 cells was partially blocked by HGF cotreatment (data not shown). TGF-β-induced growth arrest is attributed in part to the induction of a tumor suppressor gene, $p15^{INK4B}$ (Hannon and Beach, 1994). Accordingly, we examined which phosphorylation of Smad3 involved the activity of $p15^{INK4B}$ promoter, linker or C-terminal region. For the assays, we used p15P113-luc, because the segment in human $p15^{INK4B}$ promoter was sufficient to obtain TGF-β-dependent induction (Li *et al*, 1995). Cotransfection of p15P113-luc with Smad3WT or Smad3EPSM in RGM-1 cells caused to increase the basal transcriptional activity, when compared with that in cells transfected with p15P113-luc alone (Figure 9). TGF-β treatment activated the transcription, but HGF treatment suppressed the transcriptional activity triggered by TGF-β treatment. Since Smad3EPSM revealed TGF-β-dependent phosphorylation at the C-terminal region (Furukawa *et al*., 2003), these results indicate that activation of $p15^{INK4B}$ promoter requires not linker but C-terminal phosphorylation of Smad3. Therefore, a possible mechanism for HGF suppression of the transcriptional activity is via inhibition of Smad3 phosphorylation at the C-terminal region by HGF cotreatment (Figure 1d). To support this notion, forced expression of Smad3(3S-A), in which the linker region was exclusively phosphorylated, exhibited suppressive effects on the transcription.

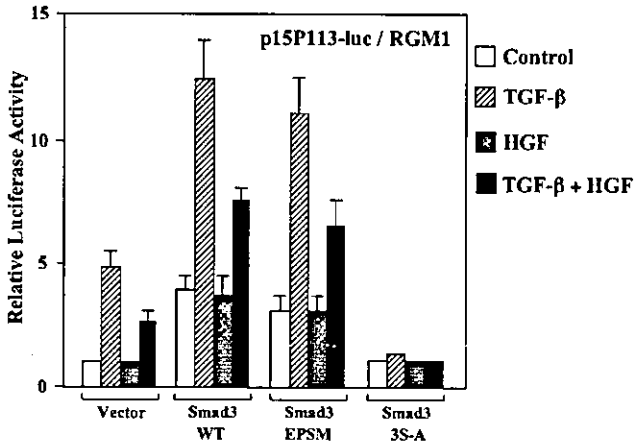

Figure 9 Activation of $p15^{INK4B}$ promoter requires not linker but C-terminal phosphorylation of Smad3. RGM-1 cells were transiently cotransfected of p15P113-luc with Smad3WT, Smad3EPSM, or Smad3(3S-A). Under serum-free conditions, the cells were incubated for 12 h with 200 pM TGF-β, 400 pM HGF, or a combination of both. Luciferase activities were determined above

Discussion

We herein described the crosstalk between receptor serine kinase and receptor tyrosine kinase signaling pathways as important implications in R-Smads-mediated signaling. Since phospho-specific Abs allow site-specific analyses in intact cells, we could focus on the domain-specific phosphorylated states of R-Smads under physiological conditions. HGF as well as TGF-β treatment activated the JNK pathway, thereafter inducing endogenous R-Smads phosphorylation at linker regions, whereas the phosphorylation at their C-terminal regions was not induced by HGF treatment. The activated JNK could directly phosphorylate R-Smads *in vitro* at the same sites that were phosphorylated in response to TGF-β or HGF *in vivo*. Thus, the linker regions of R-Smads are the common phosphorylation sites for HGF and TGF-β signaling pathways.

Nuclear translocation of Smad3 phosphorylated at the linker region by HGF stimulation strongly indicated the biological significance of the linker phosphorylation. In fact, HGF alone stimulated the invasiveness of RGM-1 cells as observed with TGF-β-stimulation, and costimulation with these two factors resulted in the additive invasive effect (Figure 7). Since JNK inhibitor suppressed these biological effects, JNK pathway could involve TGF-β and HGF-mediated infiltration potency of RGM-1 cells. In addition, our current data demonstrated that HGF treatment alone induced an activation of PAI-1 transcription, which was prominent under conditions of Smad3WT overexpression. More importantly, a combined treatment with HGF and TGF-β strongly activated PAI-1 promoter. This additional effect was dependent on Smad3 phosphorylation at the linker region by JNK pathway, because it was prevented by dominant-negative form of MEKK-1 and by transfection of Smad3EPSM. Since PAI-1 conducts the cells to migration and invasion by blocking cellular

adhesion and by promoting basement membrane degradation, stimulation of PAI-1 production might lead to an increase in invasive capacity of RGM-1 cells. Therefore, we conclude that the linker phosphorylation can participate in invasive capacity of RGM-1 cells.

The crosstalk between Smads and MAPK-mediated signals has been reported to occur in the nucleus (Wrana, 2000b). Several TGF-β-responsive elements in target genes including *PAI-1* gene contain AP1 sites. Smad3–Smad4 heteromers can form DNA binding complexes with Jun–Fos heterodimers on AP1 sites (Zhang *et al*., 1998). Another transcription factor ATF2, which is a member of the b-ZIP family of DNA binding proteins, binds to the MH1 domains of Smad3 or Smad4, and these Smads cooperate with ATF2 to activate the reporter containing cAMP response elements (Sano *et al*., 1999). Importantly, TGF-β can activate MAPKs, which in turn regulate the activity of Jun, Fos and ATF-2 and related transcription factors (Zhang and Derynck, 1999). In the nucleus, therefore, Smads interact with these proteins that are themselves targeted by MAPKs. On the other hand, our current results imply that the crosstalk already occurs at the cytoplasmic level. In the cytoplasm, JNK directly phosphorylates R-Smads, leading to the transcriptional activation of *PAI-1* gene in the nucleus.

On the other hand, receptor tyrosine kinase signaling pathway interferes with Smads to regulate TGF-β-responsive genes, resulting in antagonistic effects (Roberts *et al*., 1985). In fact, antiproliferative effect of TGF-β was partially inhibited by HGF cotreatment to RGM-1 cells. The decreased sensitivity of RGM-1 cells to the antiproliferative effect of TGF-β could be caused partly by reduced expression of the cell cycle regulator $p15^{INK4B}$, because HGF decreased transcriptional activity of $p15^{INK4B}$ induced by TGF-β (Figure 9). In addition, the induction of $p15^{INK4B}$ transcription required not linker but C-terminal phosphorylation of Smad3. Therefore, inhibitory effects of HGF on TGF-β-induced $p15^{INK4B}$ transcription could be associated with decreased phosphorylation of Smad3 at the C-terminal region by HGF cotreatment (Figure 1d). Since HGF-mediated Smad3 phosphorylation at the linker region alone promoted nuclear accumulation of Smad3, the reduction of Smad3 phosphorylation at the C-terminal region could be explained by inaccessibility of Smad3 to TβRI as a result of the preferential localization of Smad3 into the nucleus. Future work will examine whether Smad3 phosphorylated at linker region and that phosphorylated at C-terminal region differentially interact with the DNA binding partners, or recruit the transcriptional coactivators on PAI-1 and $p15^{INK4B}$ promoters.

Our present study has brought important insights into the diversity and complexity of TGF-β-mediated signal transduction. Such an arrangement may also have implications as regards the effects of TGF-β on tumor formation and progression (Wakefield and Roberts, 2002). TGF-β can act as either a tumor suppressor or a tumor promoter, depending upon the cellular context. In tumor cells that have become refractory to TGF-β-mediated growth inhibition, R-Smads phosphorylation at linker regions, in cooperation with JNK pathway, could influence tumor behavior. Consistent with the phosphorylated states of R-Smads upon HGF treatment, Smad3 highly phosphorylated at the linker region was located in the nuclei of human gastric cancerous tissues, whereas Smad2 phosphorylated at the linker region was located predominantly in the cytoplasm of the cancer cells (data not shown). In the future, identification of the phosphorylation sites in R-Smads using the specific Abs to the phosphorylated domains will reveal the molecular basis for TGF-β signaling alterations that promote the pathogenesis of human cancer.

Materials and methods

Cell culture

A rat cell line (RGM-1) was established from normal gastric mucosa (Kobayashi *et al*., 1996). The cells were cultured in Dulbecco's modified Eagle's medium with 10% fetal bovine serum and antibiotics.

Northern blot hybridization analysis

RGM-1 cells were starved for 15 h in serum-free medium, and were treated with 200 pM $TGF-\beta_1$ (R&D Systems, Minneapolis, MN, USA) and/or 400 pM HGF (R&D Systems) for 3 h. mRNAs were isolated and hybridized with labeled cDNAs probes for PAI-1 and GAPDH as described (Matsuzaki *et al*., 2000). Total RNA was isolated from cultured cells by extraction in guanidinium isothiocyanate/phenol/chloroform, and poly(A)-rich RNA was selected using oligo(dT)-cellulose (New England Biolabs Inc., Beverly, MA, USA). Aliquots (2 μg) of poly(A)-rich RNA were denatured with 2.2 M formaldehyde/50% formamide, electrophoresed through 1% agarose gels containing 2.2 M formaldehyde, and transferred onto nylon membranes (Amersham International, Buckinghamshire, UK). cDNAs were labeled with [^{32}P]dCTP (3000 Ci/mmol; Amersham International) by the random primer labeling method. The filters were hybridized with the cDNA probe in solution containing 50% formamide.

Constructs and reagents

Mammalian expression vector with an N-terminal Flag tag was constructed by inserting oligonucleotides encoding epitope-tag sequences into pcDNA3 (Invitrogen, Carlsbad, CA, USA). The coding region of Smad3 was amplified by PCR and subcloned into Flag-pcDNA3. Smad3EPSM was produced by PCR-based mutagenesis as described (Kretzschmar *et al*., 1999). PF1-Luc (Hua *et al*., 1998) was constructed by inserting the DNA fragment corresponding to −794/−532 of the PAI-1 promoter into pGL3-basic vector (Promega, Madison, WI, USA). The integrity of the constructs was confirmed by sequencing. Dominant-negative form of MEKK-1, $(SBE)_4$-luciferase reporter plasmid and p15P113-luciferase reporter plasmid were gifts from Dr S Ohno, Dr P ten Dijke, Dr X-F Wang, respectively.

Immunoprecipitation and immunoblot

To investigate effects of TGF-β and/or HGF on the phosphorylation of endogenous R-Smads, RGM-1 cells were starved for 15 h in serum-free medium, and were incubated

for 8 h in the absence or presence of 10 μM JNK inhibitor SP600125 (Calbiochem, San Diego, CA, USA) or 10 μM p38 MAPK inhibitor PD169316 (Calbiochem). The cells were then treated with 200 pM TGF-β_1 and/or 400 pM HGF for the indicated times. Following adsorption to protein-G-Sepharose (Amersham Biosciences, Piscataway, NJ, USA) with anti-Smad2/3 Ab (BD Bioscience, San Jose, CA, USA), the phosphorylation levels of R-Smads were monitored by immunoblot using each domain-specific Ab against the phosphorylated R-Smads (α pSmad2L [Ser 249/254], α pSmad2C [Ser 465/467], α pSmad3L [Ser 207/212] or α pSmad3C [Ser 423/425]) (Furukawa *et al.*, 2003; Matsuzaki *et al.*, unpublished data). To investigate heteromeric complex formation of endogenous R-Smads with endogenous Smad4, the cells were incubated for 8 h in the absence or presence of 10 μM JNK inhibitor SP600125, and were treated with 200 pM TGF-β_1 and/or 400 pM HGF for 40 min. The cell lysates were subjected to immunoprecipitation with each anti-phospho-R-Smad Ab or anti-R-Smads Ab, and Smad4 in the immunoprecipitate was monitored by immunoblot using mouse monoclonal anti-Smad4 Ab (Santa Cruz Biotechnology, Santa Cruz, CA, USA). Other immunoblots were performed using the following primary Abs: rabbit polyclonal anti-phospho-JNK1/2 Ab (Promega), rabbit polyclonal anti-phospho-p38 MAPK Ab (Promega), rabbit polyclonal anti-phospho-ERK 1/2 Ab (Promega), rabbit polyclonal anti-JNK1/2 Ab (Cell Signaling, Beverly, MA, USA), rabbit polyclonal anti-ERK1/2 Ab (Cell Signaling), and rabbit polyclonal anti-p38 Ab (Calbiochem). Samples were subjected to SDS–PAGE and then were transferred to nitrocellulose membranes (Amersham Biosciences). The blots were incubated with primary Ab for 2 h at room temperature, and then were washed three times. The appropriate secondary Ab was added for 1 h at room temperature. After washing, the immunoreactive proteins were visualized by ECL (Amersham Biosciences) and autoradiography.

In vitro *kinase assays*

Smad constructs were subcloned into pGEX-4T-1 expression vector (Amersham Biosciences) encoding an amino-terminal GST tag. Bacterial expression and purification of GST-Smad2 and GST-Smad3 were carried out according to the manufacturer's instructions (Amersham Biosciences). RGM-1 cells were starved for 15 h in serum-free medium, and were incubated with 200 pM TGF-β_1 and/or 400 pM HGF for 15 min. Endogenous kinases were isolated from the cell extracts using anti-phospho-JNK Ab (Promega). Immune complexes were collected with protein G-Sepharose and were washed four times with lysis buffer and then twice with kinase assay buffer (25 mM Tris-HCl (pH 7.5), 5 mM β-glycerophosphate, 2 mM DTT, 0.1 mM Na_3VO_4, and 10 mM $MgCl_2$). Pellets were resuspended in 50 μl of kinase assay buffer supplemented with 100 μM ATP; and 2 μg of bacterially expressed GST-Smad2 or GST-Smad3. Assays were carried out at 30°C for 30 min and then were stopped with Laemmli sample buffer. Phosphorylation sites of R-Smads were determined by immunoblot using each anti-phospho-R-Smad Ab.

Immunofluorescence study

The subcellular localization of Smads was determined as previously described (Matsuzaki *et al.*, 2000). The cells were starved for 15 h in serum-free medium, and were incubated for 8 h in the absence or presence of 10 μM JNK inhibitor SP600125. The cells were then treated with 200 pM TGF-β_1 and/or 400 pM HGF for 1 h. After fixation with 4% paraformaldehyde, the slides were incubated with a primary Ab at 4°C for 16 h. Endogenous Smad proteins were visualized with each anti-phospho-R-Smad Ab. In all cases, at least 100 stained cells were counted. Anti-pSmad3C Ab weakly cross-reacted with the C-terminally phosphorylated Smad2. To block the binding of anti-pSmad3C Ab to the phosphorylated domains in Smad2, anti-pSmad3C Ab was adsorbed with 1 μg/ml C-terminally phosphorylated Smad2 peptide.

Invasion assay

An invasion chamber with 8-μm membrane pores covered with Matrigel (BD Biosciences) was placed on a cell culture plate. RGM-1 cells (2×10^4) were cultured on Matrigel for 48 h with 200 pM TGF-β_1 and/or 400 pM HGF in the absence or presence of 10 μM JNK inhibitor SP600125. The chambers were then immersed in 100% methanol for 1 min for fixation, and all cells were then stained by hematoxylin. The cells remaining on the top surface of the membrane were completely removed with a cotton swab, and the membrane was removed from the chamber and mounted on a glass slide. These preparations were examined under a microscope at × 100 magnification. The number of infiltrating cells was counted in five regions selected at random, and the extent of invading cells was determined by the mean count. Duplicate filters were used, and the experiments were repeated three times.

Transcriptional response assay

The cells were subjected to transfection with LipofectAMINE (Invitrogen), 0.4 μg of reporter plasmid, and the indicated constructs or with an empty vector, and were incubated for 4 h. After changing the medium, the cells were incubated for a further 30 h. Under serum-free conditions, the cells were incubated for 12 h with 200 pM TGF-β_1 and/or 400 pM HGF. Finally, they were lysed, and the luciferase activities of the cell extracts were measured by a luminometer (Berthold, Bad Wildbad, Germany) using Dual-Luciferase™ Reporter Assay System (Promega). The luciferase activities were normalized based on the Renilla luciferase activity.

Abbreviations

ERK, extracellular signal-regulated kinase; JNK, c-Jun N-terminal kinase; MAPK, mitogen-activated protein kinase; MEKK-1, mitogen-activated protein kinase kinase kinase-1; PAI-1, plasminogen activator inhibitor type 1; R-Smads, receptor-regulated Smads; SAPK, stress-activated protein kinase; TAK1, TGF-β-activated kinase 1; TβRI, TGF-β type I receptor.

Acknowledgements

We would like to thank Dr R Derynck (University of California at San Francisco) and Dr S Ohno (Yokohama City University School of Medicine) for providing us with cDNAs encoding human Smad2 and Smad3 and with cDNA encoding dominant-negative form of MEKK-1, respectively. We are grateful to Dr X-F Wang (Duke University) and Drs P ten Dijke and C-H Heldin (Ludwig Institute for Cancer Research) for the generous gifts of p15P113-luc vector and $(SBE)_4$-Luc vector, respectively. We also thank Dr AB Roberts (National Cancer Institute) for helpful discussions concerned with the study. This study was supported by a Grant-in-Aid for scientific research from the Ministry of Education, Science and Culture of Japan.

References

Brown JD, DiChiara MR, Anderson KR, Gimbrone Jr MA and Topper JN. (1999). *J. Biol. Chem.*, **274**, 8797–8805.
Davis RJ. (1993). *J. Biol. Chem.*, **268**, 14553–14556.
de Caestecker MP, Parks WT, Frank CJ, Castagnino P, Bottaro DP, Roberts AB and Lechleider RJ. (1998). *Genes Dev.*, **12**, 1587–1592.
Derynck R, Zhang Y and Feng XH. (1998). *Cell*, **95**, 737–740.
Engel ME, McDonnell MA, Law BK and Moses HL. (1999). *J. Biol. Chem.*, **274**, 37413–37420.
Furukawa F, Matsuzaki K, Mori S, Tahashi Y, Yoshida K, Sugano Y, Yamagata H, Matsushita M, Seki T, Inagaki Y, Nishizawa M, Fujisawa J and Inoue K. (2003). *Hepatology*, **38**, 879–889.
Gutierrez LS, Schulman A, Brito-Robinson T, Noria F, Ploplis VA and Castellino FJ. (2000). *Cancer Res.*, **60**, 5839–5847.
Hannon GJ and Beach D. (1994). *Nature*, **371**, 257–261.
Heldin CH, Miyazono K and ten Dijke P. (1997). *Nature*, **390**, 465–471.
Hill CS and Treisman R. (1995). *Cell*, **80**, 199–211.
Hirashima Y, Kobayashi H, Suzuki M, Tanaka Y, Kanayama N and Terao T. (2003). *J. Biol. Chem.*, **278**, 26793–26802.
Hua X, Liu X, Ansari DO and Lodish HF. (1998). *Genes Dev.*, **12**, 3084–3095.
Jonk LJ, Itou S, Heldin CH, ten Dijke P and Kruijer W. (1998). *J. Biol. Chem.*, **273**, 21145–21152.
Kimelman D and Kirschner M. (1987). *Cell*, **51**, 869–877.
Kobayashi I, Kawano S, Tsuji S, Matsui H, Nakama A, Sawaoka H, Masuda E, Takei Y, Nagano K, Fusamoto H, Ohno T, Fukutomi H and Kamada T. (1996). *In Vitro Cell Dev. Biol. Anim.*, **32**, 259–261.
Kretzschmar M, Doody J and Massagué J. (1997). *Nature*, **389**, 618–622.
Kretzschmar M, Doody J, Timokhina I and Massagué J. (1999). *Genes Dev.*, **13**, 804–816.
Li J-M, Nichols MA, Chandrasekharan S, Xiong Y and Wang X-F. (1995). *J. Biol. Chem.*, **270**, 26750–26753.
Macías-Silva M, Abdollah S, Hoodless PA, Pirone R, Attisano L and Wrana JL. (1996). *Cell*, **87**, 1215–1224.
Massagué J. (1998). *Annu. Rev. Biochem.*, **67**, 753–791.
Matsuzaki K, Date M, Furukawa F, Tahashi Y, Matsushita M, Sakitani K, Yamashiki N, Seki T, Saito H, Nishizawa M, Fujisawa J and Inoue K. (2000). *Cancer Res.*, **60**, 1394–1402.
Mulder KM. (2000). *Cytokine Growth Factor Rev.*, **11**, 23–35.
Nakao A, Afrakhte M, Morén A, Nakayama T, Christian JL, Heuchel R, Itoh S, Kawabata M, Heldin NE, Heldin CH and ten Dijke P. (1997). *Nature*, **389**, 631–635.
Piek E, Ju WJ, Heyer J, Escalante-Alcalde D, Stewart CL, Weinstein M, Deng C, Kucherlapati R, Bottinger EP and Roberts AB. (2001). *J. Biol. Chem.*, **276**, 19945–19953.
Roberts AB, Anzano MA, Lamb LC, Smith JM and Sporn MB. (1981). *Proc. Natl. Acad. Sci. USA*, **78**, 5339–5343.
Roberts AB, Anzano MA, Wakefield LM, Roche NS, Stern DF and Sporn MB. (1985). *Proc. Natl. Acad. Sci. USA*, **82**, 119–123.
Roberts AB and Sporn MB. (1990). *Peptide Growth Factors and Their Receptors, Part I, Vol 95* Sporn MB and Roberts AB. (eds). Springer-Verlag: Berlin, pp. 419–472.
Robinson MJ and Cobb MH. (1997). *Curr. Opin. Cell Biol.*, **9**, 180–186.
Sano Y, Harada J, Tashiro S, Gotoh-Mandeville R, Maekawa T and Ishii S. (1999). *J. Biol. Chem.*, **274**, 8949–8957.
Schlessinger J. (2002). *Cell*, **110**, 669–672.
Stoker M, Gherardi E, Perryman M and Gray J. (1987). *Nature*, **327**, 239–242.
Wakefield LM and Roberts AB. (2002). *Curr. Opin. Genet. Dev.*, **12**, 22–29.
Wrana JL. (2000a). *Cell*, **100**, 189–192.
Wrana JL. (2000b). *Sci. STKE*, **2000**, RE1.
Yamaguchi K, Shirakabe K, Shibuya H, Irie K, Oishi I, Ueno N, Taniguchi T, Nishida E and Matsumoto K. (1995). *Science*, **270**, 2008–2011.
Zhang Y, Feng XH and Derynck R. (1998). *Nature*, **394**, 909–913.
Zhang Y and Derynck R. (1999). *Trends Cell Biol.*, **9**, 274–279.

IgA Class Switch Occurs in the Organized Nasopharynx- and Gut-Associated Lymphoid Tissue, but Not in the Diffuse Lamina Propria of Airways and Gut[1]

Takashi Shikina,*† Takachika Hiroi,*‡¶ Kohichi Iwatani,* Myoung Ho Jang,* Satoshi Fukuyama,*¶ Manabu Tamura,† Takeshi Kubo,† Hiromichi Ishikawa,§ and Hiroshi Kiyono[2]*‡¶

Secretory IgA plays a crucial role in the host immune response as a first line of defense. A recent demonstration of in situ IgA class switching in intestinal lamina propria provided an opportunity to reconsider the model for the homing of IgA-committed B cells characterized by distinctive trafficking patterns to effector sites. Those effector sites depend on the organized mucosa-associated lymphoid tissues as their site of induction. In this report we show the preferential presence of IgM^+B220^+ and IgA^+B220^+ cells belonging to pre- and post-IgA isotype class-switched cells in the organized mucosa-associated lymphoid tissues, such as nasopharynx-associated lymphoid tissues, isolated lymphoid follicles, and Peyer's patches, and the defect of those populations in the diffuse effector tissues, such as the nasal passage and intestinal lamina propria. Consistent with these findings, the expressions of a series of IgA isotype class switch recombination-related molecules, including activation-induced cytidine deaminase, Iα-Cμ circle transcripts, and Iα-Cμ circle transcripts, were selectively detected in these organized mucosa-associated lymphoid structures, but not in the diffuse mucosal effector sites. Taken together, these findings suggest that IgA isotype class switching occurs only in the organized mucosa-associated lymphoid organs (e.g., nasopharynx-associated lymphoid tissues, isolated lymphoid follicles, and Peyer's patches), but not in the diffuse effector tissues of the upper respiratory and gastrointestinal tracts. ***The Journal of Immunology,*** **2004, 172: 6259–6264.**

The mucosal immune system provides the first line of defense against the ingress of microbial pathogens during the physiological processes of inhalation and ingestion. One of the major components of the mucosal immune system is secretory IgA (S-IgA),[3] which is produced by the mucosal interaction of epithelial cells, IgA-committed B cells, and Th cells in the respiratory and gastrointestinal tracts (1, 2). Thus, mucosal effector sites such as the lamina propria of the upper respiratory and intestinal tract contain high numbers of IgA blast and plasma cells derived from postswitched IgA^+ B cells.

IgA-committed B cells that have undergone μ to α isotype class switching in nasopharynx-associated lymphoid tissue (NALT), Peyer's patches (PPs), and other mucosal inductive lymphoid organs are generally believed to migrate to diffuse mucosal effector tissues, including the nasal passage (NP) and intestinal lamina propria (i-LP) (3, 4). PPs show a high frequency of IgM^+ $B220^+$ B cells, which are a prerequisite for isotype class switching to IgA^+B220^+ B cells after antigenic or mitogenic stimulation in the presence of the isotype switch-inducing cytokine TGF-β (1, 5–8). PPs are an example of organized gut-associated lymphoid tissue (GALT) with germinal centers (GCs) and are thus considered to be a major site for the μ to α class switch recombination (CSR) involving activation-induced cytidine deaminase (AID), Iα-Cμ circle transcripts (αCTs), and Iμ-Cα transcripts (9, 10). Recent results, generated from analysis of AID-deficient mice, however, have suggested another pathway for the development of intestinal IgA plasma cells (11). IgA class switching was shown to occur in i-LP without the involvement of PPs or other organized mucosa-associated lymphoid tissues (MALT) containing GCs. In this study, IgM^+ $B220^+$ B cells in i-LP switched to IgA^+ B cells under the influence of TGF-β derived from i-LP stromal cells (11). These findings suggest that i-LP could have the immunological function of both effector and inductive sites. However, the concerns with that study were that the researchers did not have control of the compartment from which the B cells were harvested, either the diffuse lamina propria or isolated lymphoid follicles (ILFs) embedded in the lamina propria, due to the nature of AID-deficient mice. Because $AID^{-/-}$ mice exhibited enormous hyperplasia of ILFs, there was little of the diffuse lamina propria region left (11).

We recently identified ILFs as part of the organized GALT in mouse small intestine (12). ILFs are comprised of a single B cell

*Department of Mucosal Immunology, Research Institute for Microbial Diseases, Osaka University, Osaka, Japan; †Department of Otolaryngology and Sensory Organ Surgery, Osaka University Graduate School of Medicine, Osaka, Japan; ‡Core Research for Engineering, Science, and Technology, Japan Science and Technology Corp., Tokyo, Japan; §Department of Microbiology and Immunology, Keio University School of Medicine, Tokyo, Japan; and ¶Division of Mucosal Immunology, Institute of Medical Science, University of Tokyo, Tokyo, Japan

Received for publication October 9, 2003. Accepted for publication March 11, 2004.

The costs of publication of this article were defrayed in part by the payment of page charges. This article must therefore be hereby marked *advertisement* in accordance with 18 U.S.C. Section 1734 solely to indicate this fact.

[1] This work was supported by grants-in-aid from Core Research for Engineering, Science, and Technology of Japan Science and Technology Corp.; the Ministry of Education, Science, Sports, and Culture of Japan; the Ministry of Health, Labor, and Welfare of Japan; and the Japanese Human Science Foundation.

[2] Address correspondence and reprint requests to Dr. Hiroshi Kiyono, Division of Mucosal Immunology, Institute of Medical Science, University of Tokyo, 4-6-1 Shirokanedai, Minato-Ku, Tokyo 108-8639, Japan. E-mail address: kiyono@ims.u-tokyo.ac.jp

[3] Abbreviations used in this paper: S-IgA, secretory IgA; AID, activation-induced cytidine deaminase; CSR, class switch recombination; CT, cholera toxin; αCT, Iα-Cμ circle transcript; GALT, gut-associated lymphoid tissue; GC, germinal center; ILF, isolated lymphoid follicle; i-LP, intestinal lamina propria; MC, mononuclear cell; MLN, mesenteric lymph node; NALT, nasopharynx-associated lymphoid tissue; NP, nasal passage; PP, Peyer's patch

0022-1767/04/$02.00

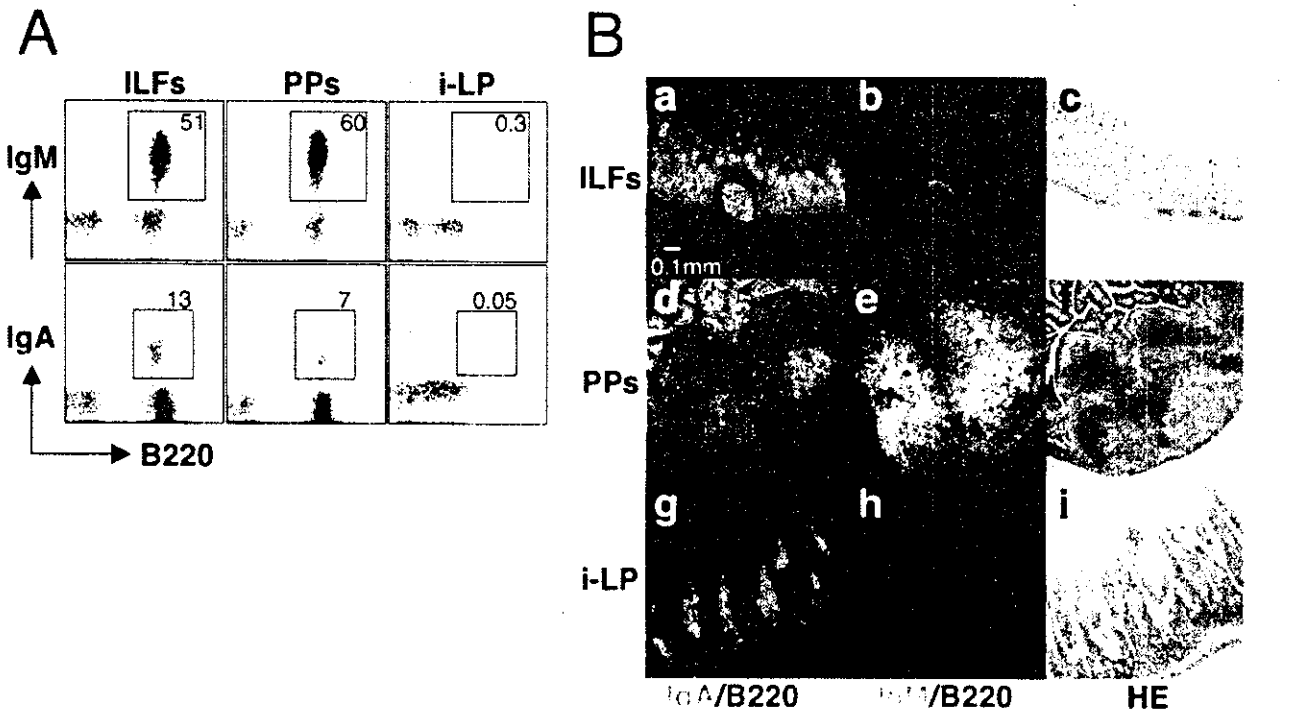

FIGURE 1. The accumulation of IgM$^+$B220$^+$ and IgA$^+$B220$^+$ cells in ILFs and PPs and their absence in the i-LP of mouse small intestine. *A*, MCs isolated from ILFs, PPs, and i-LP were stained with a panel of mAbs specific for IgM, IgA, and B220. The i-LP MCs were prepared after complete removal of ILFs and PPs. *B*, Consecutive tissue sections were stained with FITC-conjugated anti-IgA (*a*, *d*, and *g*), anti-IgM (*b*, *e*, and *h*), and PE-conjugated anti-B220 (*a*, *b*, *d*, *e*, *g*, and *h*). These tissues were also stained with HE (*c*, *f*, and *i*). Although cells expressing IgA or IgM (green) as well as those expressing B220 (red) were found in ILFs and PPs (*a*, *b*, *d*, and *e*), double-positive cells were hardly detected in i-LP (*g* and *h*), where IgA$^+$B220$^-$ blast/plasma cells (green) were abundant (*g*). These sections were analyzed by confocal microscopy using a ×25 magnification. Results are representative of three separate experiments.

follicle with GCs overlaid by a follicle-associated epithelium containing Ag up-taking M cells that are similar to the follicle-associated epithelium of PPs. The presence of ILF tissue could provide additional mucosal inductive sites for the generation of IgA-committed B cells in the gastrointestinal tract (13). In fact, looking at the data overall, it is not possible to exclude the possibility that ordinary preparations of i-LP samples may contain IgM$^+$ B220$^+$ B cell fractions undergoing in situ class switching inside the GCs of these newly discovered murine ILFs (12).

For the upper respiratory tract, NALT has been shown to contain all the necessary molecular and cellular environments for the initiation of IgA B cell responses (2, 14, 15). NALT has also been identified as a region in which both IgA-committed B cells and memory-type IgA$^+$ B cells are generated (15). Nasal immunization has been shown to effectively induce Ag-specific IgA Ab responses via NALT for the upper respiratory tract, including the NP (2, 16). Thus, in the respiratory tract, NALT, with its inductive sites, and NP, with its effector sites, are considered to be part of the IgA-committed B cell-homing pathway analogous with PPs and i-LP in the gastrointestinal tract.

In this study, using the molecular and cellular analyses of transcription as well as immunocytochemistry and immunohistochemistry, NALT and GALT, including ILFs and PPs as well as NP and i-LP, were examined as examples of organized inductive and diffuse effector tissues, respectively. In this paper we report evidence that organized MALT, but not the diffuse lamina propria of the respiratory and intestinal tracts, play an essential role in the generation of IgA-committed B cells, especially in the μ to α isotype class switching for the mucosal immune system.

Materials and Methods

Mice

BALB/c mice were purchased from CLEA Japan (Tokyo, Japan) and used at 6–12 wk of age. In some experiments mice were nasally immunized with

Table I. *Distribution of different B cell subsets in organized mucosa inductive vs diffuse effector tissues*[a]

B Cell Subsets		Respiratory Tract		Intestinal Tract		
				Inductive		
sIg	B220	Inductive, NALT	Effector, NP	ILFs	PPs	Effector, i-LP
IgM	+	46.75 ± 0.19	0.53 ± 0.1	49.6 ± 5.8	63.9 ± 4.9	0.31 ± 0.11
IgA	+	0.79 ± 0.59	0.06 ± 0.01	11.3 ± 3.1	8.2 ± 1.7	0.06 ± 0.04
IgA	−	0.20 ± 0.14	7.69 ± 1.2	1.9 ± 0.8	0.5 ± 0.2	21.7 ± 5.3

[a] MCs were isolated from the organized inductive and effector tissues of the respiratory and intestinal tracts for flow cytometric analysis with fluorochrome-conjugated mAbs anti-μ, anti-α, and PE-conjugated mAb anti-B220. The percentages of the B cell subset indicated in the *left column* in various tissues are shown in each row. The data are presented as the mean ± SD from three separate experiments. sIg, surface Ig.

1 μg of cholera toxin (CT; Sigma-Aldrich, St. Louis, MO), a potent immunogen with strong adjuvanticity (17), once a week for 3 consecutive wk (16).

Cell preparation

Mononuclear cells (MCs) were isolated from spleen, PPs, NP, and NALT as described previously (16, 18). MCs from spleen and NALT were obtained using a mechanical dissociation procedure (16, 18). MCs from PPs and NP were prepared using the enzymatic dissociation protocol with collagenase D (Roche, Mannheim, Germany) (16, 18). MCs from ILFs were prepared as described previously (12). In brief, the small intestine was opened longitudinally along the mesenteric wall. After removal of mucus and feces, an intestinal fragment ~3 cm in length was pasted on a culture dish. Under a transillumination stereomicroscope (TH3; Olympus, Tokyo, Japan), a tiny fragment of the small intestine containing a single ILF was amputated by a sharpened needle. After removal of PPs and ILFs, i-LP lymphocytes were isolated from the small intestine by the enzymatic dissociation procedure with collagenase D (Roche) (18).

Flow cytometry

FITC-conjugated anti-mouse IgA and IgM, and R-PE-conjugated anti-B220 were used for staining (BD PharMingen, San Jose, CA) (18). MCs isolated from different tissues were preincubated with Fc Block (2 μg/ml; BD PharMingen) before fluorochrome-conjugated mAbs. MCs were then incubated with optimal concentrations of FITC-conjugated anti-mouse IgA (2 μg/ml) or IgM (2 μg/ml) together with PE-conjugated anti-B220 (2 μg/ml). Flow cytometric analysis was then performed using FACSCalibur (BD Biosciences, San Jose, CA) (18).

Immunohistochemical analysis

Vertically oriented sections of the small intestine that included PPs and/or ILFs as well as NP and NALT were prepared as previously described (2, 12). Briefly, the small intestine was longitudinally opened along the mesenteric wall, rolled up, and frozen in OCT compound (Sakura Finetechnical, Tokyo, Japan) in liquid nitrogen. Serial frozen sections were then incubated with FITC-conjugated anti-IgA (2 μg/ml) or FITC-conjugated anti-IgM (2 μg/ml) and PE-conjugated anti-B220/CD45R (2 μg/ml; all from BD PharMingen) for 1 h at room temperature. The slides were then examined using confocal microscopy (Bio-Rad, Hercules, CA). After confocal fluorescence microscopic analysis, the sections were counterstained with H&E. The sections used for examination were prepared from at least three individual mice.

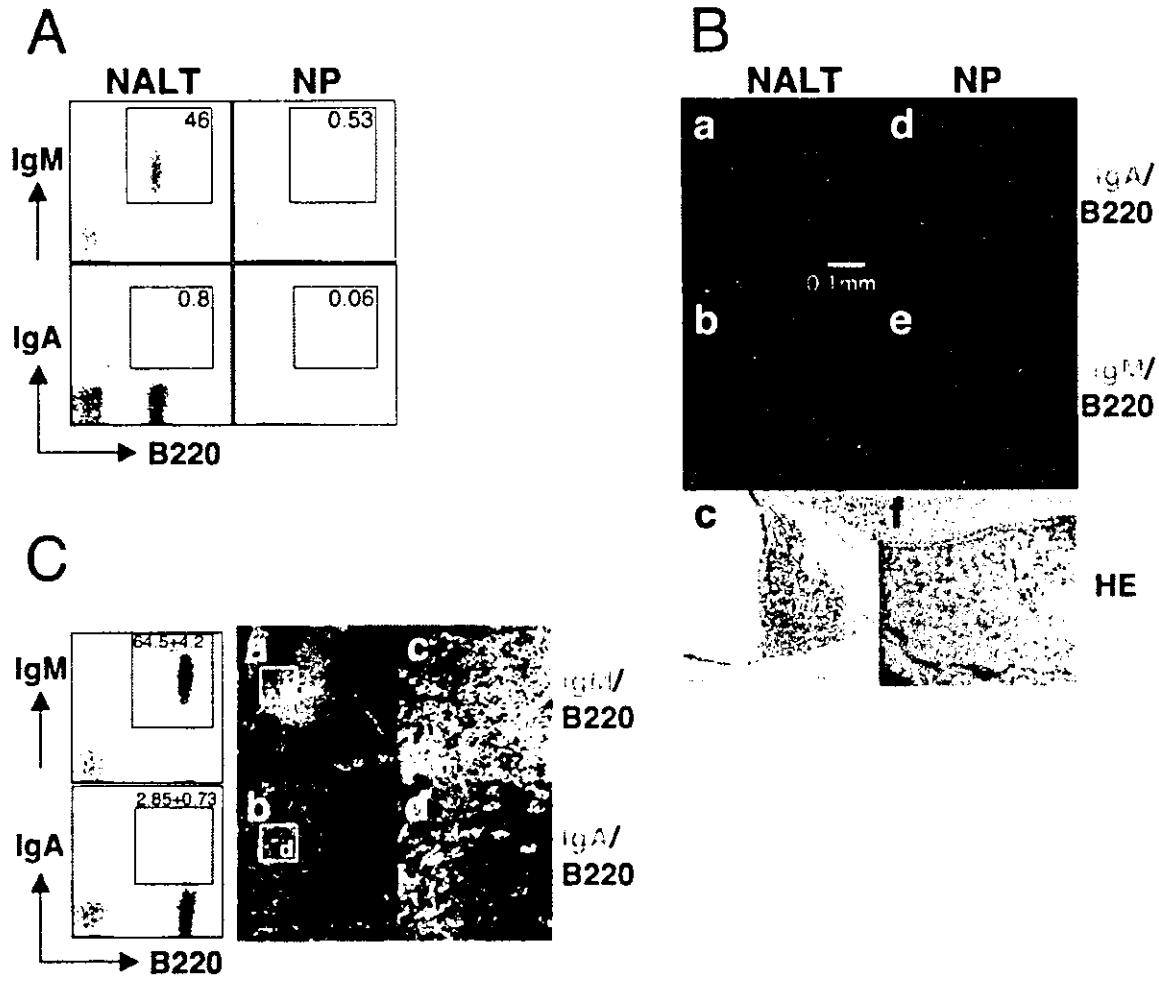

FIGURE 2. Selective localization of IgM^+B220^+ cells in NALT, but not in NP. *A*, MCs isolated from NALT and NP were stained with a panel of mAbs specific for IgM, IgA, and B220. *B*, Consecutive tissue sections were stained with FITC-conjugated anti-IgA (*a* and *d*), anti-IgM (*b* and *e*), and PE-conjugated anti-B220 (*a*, *b*, *d*, and *e*). Samples of each tissue were also stained with HE (*c* and *f*). Cells expressing IgA or IgM (green) as well as those expressing B220 (red) were found only in NALT (*a* and *b*). The numbers of double-positive cells (yellow) of IgA or IgM and B220 were negligible (*d* and *e*), although IgA^+B220^- blasts and plasma cells were plentiful (*d*). *C*, IgA^+ $B220^+$ B cells increased in NALT after nasal immunization with CT. MCs isolated from NALT were stained with a panel of mAbs specific for IgM, IgA, and B220. Consecutive tissue sections were stained with FITC-conjugated anti-IgM and PE-conjugated anti-B220 (*a*) or FITC-conjugated anti-IgA and PE-conjugated anti-B220 (*b*). Higher magnification of sections *a* and *b* are shown in *c* and *d*, respectively. Double-positive cells (yellow) for IgA (green) and B220 (red) were increased in NALT (*C-b* or *C-d*) after nasal immunization with CT (0.8–2.9%). In contrast, double-positive cells (yellow) for IgM (green) and B220 (red) were found in both naive and immunized NALT (*B-b* and *C-a* or *C-c*). These sections were analyzed by confocal microscopy using ×35 (*B*, *C-a*, and *C-b*) and ×200 (*C-c* and *C-d*) magnifications. Results are representative of three separate experiments.

RT-PCR

Total RNA isolated from mouse tissues was extracted, following the manufacturer's instructions, using TRIzol (Invitrogen, Carlsbad, CA). cDNA was prepared by reverse transcriptase (Invitrogen) with oligo(dT) primer. AID transcripts, αCTs, Iμ-Cα, and β-actin transcripts were amplified as described previously (9–11). The oligonucleotide primers specific for AID transcripts (5′-GGCTGAGGTTAGGGTTCCATCTCAG-3′ and 5′-GAGG GAGTCAAGAAAGTCACGCTGGA-3′), Iα-Cμ circle transcripts (5′-CCAGGCATGGTTGAGATAGAGATAG-3′ and 5′-AATGGTGCTGGG CAGGAAGT-3′), Iμ-Cα transcripts (5′-CTCTGGCCCTGCTTATTGT TG-3′ and 5′-GAGCTGGTGGGAGTGTCAGTG-3′), and β-actin transcripts (5′-TGGAATCCTGTGGCATCCATGAAAC-3′ and 5′-TAAAACGCAGC TCAGTAACAGTCCG-3′) were prepared according to previously described methods (9–11). The experiments were conducted on three separate occasions.

Results

Focal accumulation of IgM^+B220^+ and IgA^+B220^+ cells in organized GALT structures, but not diffuse effector tissues

To investigate the exact class-switching sites in different parts of the wall of the mouse small intestine, we initially examined and compared the localized presence of IgM^+B220^+ B cells, which are considered to be prerequisite for class switching recombination (19, 20). To accomplish this goal, careful separation of the organized lymphoid tissue and the diffuse effector tissue was required. GALT, including PPs and especially ILFs, was carefully identified and removed. After the removal of GALT, but before enzymatic dissociation, the intestine was further re-examined, using microscopic analysis, to ensure and confirm the complete removal of organized lymphoid tissue. Screening for IgM^+B220^+ B cells revealed their presence in ILFs and PPs, but their almost complete absence from i-LP (Fig. 1*A* and Table I). Furthermore, because IgA^+B220^+ B cells are believed to result from recent class switching involving the expression of CSR molecules such as AID and looped-out circular DNA (11), we next screened for the presence of IgA^+B220^+ B cells in these different intestinal mucosa-associated tissues. Although FACS analysis revealed the presence of IgA^+B220^+ B cells in ILFs and PPs, hardly any were detected in i-LP (Fig. 1*A* and Table I). Furthermore, the preferential localization of both IgM^+B220^+ cells and IgA^+B220^+ B cells in the organized lymphoid tissues was also revealed by immunohistochemical analysis using fluorescence confocal microscopy (Fig. 1*B*). By contrast, both populations were absent in diffuse i-LP regions. Instead, larger numbers of IgA^+B220^- B cells, corresponding to the blast and plasma stages, were found in diffuse effector tissues (Table I). Taken together, these observations suggest that the isotype class switching of B cells from μ- to α-chains occurs selectively in the organized lymphoid structure of ILFs and PPs, but not in the diffuse effector tissues of i-LP of the small intestine.

In the upper respiratory tract, IgM^+B220^+ and IgA^+B220^+ B cells are present in NALT, but not in NP

In the generation of IgA-committed B cells, NALT has been shown to be as important an inductive site as GALT (1, 15, 16). When similar evaluation of the respiratory mucosal immune system for IgM^+B220^+ B cell presence was conducted, the tissue localization pattern was similar to that we described for the intestinal tract. Thus, IgM^+B220^+ B cells were preferentially localized in the organized NALT, but were virtually absent from the diffuse effector tissues of the NP (Fig. 2, *B-b* or *B-e*, and Table I). In contrast to PPs and ILFs, extremely few IgA^+B220^+ B cells were found in NALT (Fig. 2*B-a* and Table I). Ag stimulation by bacterial flora of the upper respiratory tract is weaker than that by gut flora surrounding GALT, and we hypothesized that this was the reason for the lack of IgA^+B220^+ B cells in NALT. To test this hypothesis we performed nasal immunization with CT, which is known to possess a strong antigenicity with potent mucosal adjuvant activity (17). After nasal immunization, the presence of IgA^+B220^+ B cells increased in NALT (Fig. 2*C* and Table II). The formation of GCs and the accumulation of IgA^+B220^+ B cells were also seen in the NALT of these nasally immunized mice (Fig. 2*C*). These results demonstrate that in the upper respiratory tract, IgA isotype class switching occurs in the organized NALT, but not in the diffuse lamina propria of the NP.

Table II. *Influence of nasal CT on the development of IgA^+ B cells in NALT*[a]

B Cell Subsets		Nasal Immunization	
sIg	B220	Before	After
IgM	+	54.8 ± 6.90	64.5 ± 4.2
IgA	+	0.93 ± 0.72	2.85 ± 0.73
IgA	−	0.04 ± 0.02	0.48 ± 0.09

[a] After nasal immunization with CT, which is known to possess a strong antigenicity with potent mucosal adjuvant activity, MCs were isolated from NALT and then analyzed by flow cytometry with fluorochrome-conjugated mAbs anti-μ, anti-α, or PE-conjugated mAb anti-B220. Percentages of the B cell subset indicated in the *left column* in NALT before and after nasal immunization with CT are shown in each row. The data are presented as the mean ± SD from three separate experiments. sIg, surface Ig.

Expression of CSR-associated mRNA observed in the organized MALT structure, but not in diffuse effector tissues

To test for CSR from the μ-chain to the α-chain at the molecular level, three molecular markers, AID, αCTs, and Iμ-Cα, were selected. AID was essential for CSR and completely regulated stimulated B cells undergoing class switching (9–11). αCTs were produced from circular DNA that is looped out and lost after CSR (9–11). Iμ-Cα transcripts were produced from α germline transcripts after looping out of αCTs (9–11). Because the expression of AID and αCTs is strictly up-regulated during and is quickly down-regulated after isotype class switching, such expression is considered to characterize the class switching of B cells from μ to α (10). Meanwhile, Iμ-Cα transcripts were seen to be expressed immediately after completion of IgA-specific CSR (11). To further confirm that IgA isotype class switching occurs in vivo at the organized MALT, we next used RT-PCR analysis to test for the expression of CSR-associated molecules, including AID, αCTs,

FIGURE 3. Preferential presence of AID, αCT, and Iμ-Cα transcripts in the organized lymphoid tissues of NALT, PPs, and ILFs, but not in the diffuse effector tissues of NP and i-LP. RT-PCR analysis revealed AID, αCT, and Iμ-Cα transcripts in NALT, PPs, and ILFs, but not in i-LP and NP. As a negative control for RT-PCR, the total RNA of MCs isolated from spleen of recombinase-activating gene-1(RAG1)$^{-/-}$ mice was used. The experiments were conducted on three separate occasions.

and Iμ-Cα transcripts, in the organized lymphoid and diffuse effector tissues of the gastrointestinal and respiratory tracts. The results were consistent with our finding of histological localization of IgM^+B220^+ B cells and IgA^+B220^+ B cells (Figs. 1 and 2, and Tables I and II). mRNA expressions of AID, αCTs, and Iμ-Cα transcripts were restricted to the organized MALT, such as ILFs, PPs, and NALT, but were not found in the diffuse effector tissues of i-LP and NP (Fig. 3). These results indicate that IgA isotype class switching selectively occurs in the organized MALT, but not in the diffuse effector tissues.

Discussion

PPs have been shown to contain all the cellular and microarchitectural environments (e.g., B cell follicle, including GCs, follicular dendritic cells network, and interfollicular T cell area) needed for the generation of IgA-committed B cells (1). A large number of IgM^+B220^+ B cells in the GCs of PP follicles express AID and undergo the molecular event of μ to α isotype class switching (9). Results have shown that the incubation of IgM^+ IgA^- B cells isolated from PPs together with TGF-β results in the induction of IgA isotype class switching, which leads to the generation of IgM^-IgA^+ B cells (5–8). After generation in PPs, these postswitched IgA^+ B cells (or IgA-committed B cells) migrate to effector tissues, such as i-LP, where they become IgA blast and plasma cells under the influence of IgA-enhancing cytokines IL-5, IL-6, and IL-10 (1). Therefore, it is generally accepted that organized MALT, such as PPs, acting as inductive sites, play a major role in the initiation of the IgA Ab response, while diffuse i-LP tissues provide the effector sites (1). This conjecture was further confirmed by our current results, which show that IgM^+B220^+ B cells capable of undergoing μ to α isotype class switching were exclusively located in PPs and were absent from diffuse i-LP. In contrast, large numbers of IgA blast and plasma cells were found in these diffuse i-LP. Furthermore, evaluation of CSR-associated molecules for the μ to α gene rearrangement revealed that AID, αCTs, and Iμ-Cα transcripts were selectively expressed in PPs with the organized lymphoid structure, but not in the diffuse i-LP.

In addition to testing PPs, we tested ILFs, which we recently characterized as part of the organized GALT on the antimesenteric wall of the mouse small intestine (12). This cell formation is composed of a large B cell area, including GCs. A large fraction of the B cells in ILFs are B-2 cells, similar to those found in PPs (12). In this study our findings further demonstrate that ILFs are a rich source of IgM^+B220^+ B cells that can undergo μ to α CSR. Thus, CSR-associated transcripts of AID, αCT, and Iμ-Cα were present in the mRNA preparation obtained from ILF as well as PP samples. After careful removal of ILFs and PPs, MCs that had been isolated from the diffuse effector tissues of i-LP were evaluated for the IgA-associated CSR-associated transcripts. No AID, αCT, or Iμ-Cα transcripts were found in the diffuse tissue of i-LP. Taken together, these findings indicate that ILFs and PPs, both of which contain B cell follicles with GCs, constitute the organized GALT and behave as key inductive sites for μ to α isotype class switching when IgA-committed B cells are generated.

When we evaluated the presence and population density of IgM^+ B cells and/or IgA^+ B cells in different histological locations of the upper respiratory tract, accumulations of IgM^+B220^+ B cells were always observed only in the organized MALT such as NALT. These cells were absent in the NP, a representative diffuse effector site for the upper respiratory tract (Fig. 2 and Table I). In addition, AID, αCT, and Iμ-Cα transcripts were expressed in NALT, but not in NP, paralleling expression by ILFs and PPs, but not i-LP, in the intestinal tract (Fig. 3). Previously we have shown that NALT B cells belong to a subset of B-2 cells (18). That study also showed that IgA isotype class switching of B-2 cells in the upper respiratory tract occurs only in the organized MALT, such as NALT, and not in the diffuse lamina propria region of the NP.

Comparisons of NALT and GALT (e.g., ILFs and PPs) for the population density of switched IgA^+B220^+ B cells revealed a dramatic difference. Much higher numbers of IgA^+B220^+ B cells were found in GALT (e.g., 6.5–14.4%; Table I) than in NALT (e.g., 0.2–1.4%; Table I). That finding may be explained by the different microbial environments found in NALT and GALT. In comparison with NALT, GALT structures are situated in a part of the gut where there is an enormous load of microbial Ags and mitogens to continuously stimulate immunocompetent cells located in the organized lymphoid tissue for the mucosal immune system. Thus, administration of CT possessing potent immunogenicity and adjuvanticity via the nasal route resulted in a 3- to 10-fold increase in the population (e.g., 2.9 ± 0.7%; Fig. 2). This increase points to the importance of antigenic stimulation in the initiation of IgA class isotype switching for the generation of IgA-committed B cells in NALT. Elsewhere, we have shown that the tissue organogenesis of NALT is also accelerated by nasal exposure to Ag (21).

Acknowledgments

We thank Noriko Kitagaki for her technical help, and the members of the Mucosal Immunology Group of Osaka University for their critical comments. We also thank Misako Hashimoto for her secretarial assistance.

References

1. Mestecky, J., R. S. Blumberg, H. Kiyono, and J. R. McGhee. 2003. The mucosal immune system. In *Fundamental Immunology*, 4th Ed. W. E. Paul, ed. Lippincott Williams & Wilkins, Philadelphia, p. 465.
2. Hiroi, T., K. Iwatani, H. Iijima, S. Kodama, M. Yanagita, and H. Kiyono. 1998. Nasal immune system: distinctive Th0 and Th1/Th2 type environments in murine nasal-associated lymphoid tissues and nasal passage, respectively. *Eur. J. Immunol. 28:3346.*
3. Brandtzaeg, P., I. N. Farstad, and G. Haraldsen. 1999. Regional specialization in the mucosal immune system: primed cells do not always home along the same track. *Immunol. Today 20:267.*
4. Kunkel, E. J., and E. C. Butcher. 2003. Plasma-cell homing. *Nat. Rev. Immunol. 3:822.*
5. Coffman, R. L., D. A. Lebman, and B. Shrader. 1989. Transforming growth factor β specifically enhances IgA production by lipopolysaccharide-stimulated murine B lymphocytes. *J. Exp. Med. 170:1039.*
6. Ehrhardt, R. O., W. Strober, and G. R. Harriman. 1992. Effect of transforming growth factor (TGF)-β1 on IgA isotype expression. TGF-β1 induces a small increase in $sIgA^+$ B cells regardless of the method of B cell activation. *J. Immunol. 148:3830.*
7. Sonoda, E., Y. Hitoshi, N. Yamaguchi, T. Ishii, A. Tominaga, S. Araki, and K. Takatsu. 1992. Differential regulation of IgA production by TGF-β and IL-5: TGF-β induces surface IgA-positive cells bearing IL-5 receptor, whereas IL-5 promotes their survival and maturation into IgA-secreting cells. *Cell. Immunol. 140:158.*
8. Kim, P. H., and M. F. Kagnoff. 1990. Transforming growth factor-β1 is a co-stimulator for IgA production. *J. Immunol. 144:3411.*
9. Muramatsu, M., V. S. Sankaranand, S. Anant, M. Sugai, K. Kinoshita, N. O. Davidson, and T. Honjo. 1999. Specific expression of activation-induced cytidine deaminase (AID), a novel member of the RNA-editing deaminase family in germinal center B cells. *J. Biol. Chem. 274:18470.*
10. Kinoshita, K., M. Harigai, S. Fagarasan, M. Muramatsu, and T. Honjo. 2001. A hallmark of active class switch recombination: transcripts directed by I promoters on looped-out circular DNAs. *Proc. Natl. Acad. Sci. USA 98:12620.*
11. Fagarasan, S., K. Kinoshita, M. Muramatsu, K. Ikuta, and T. Honjo. 2001. In situ class switching and differentiation to IgA-producing cells in the gut lamina propria. *Nature 413:639.*
12. Hamada, H., T. Hiroi, Y. Nishiyama, H. Takahashi, Y. Masunaga, S. Hachimura, S. Kaminogawa, H. Takahashi-Iwanaga, T. Iwanaga, H. Kiyono, et al. 2002.

Identification of multiple isolated lymphoid follicles on the antimesenteric wall of the mouse small intestine. *J. Immunol. 168:57.*

13. Brandtzaeg, P., E. S. Baekkevold, and H. C. Morton. 2001. From B to A the mucosal way. *Nat. Immunol. 2:1093.*
14. Wu, H. Y., H. H. Nguyen, and M. W. Russell. 1997. Nasal lymphoid tissue (NALT) as a mucosal immune inductive site. *Scand. J. Immunol. 46:506.*
15. Csencsits, K. L., M. A. Jutila, and D. W. Pascual. 1999. Nasal-associated lymphoid tissue: phenotypic and functional evidence for the primary role of peripheral node addressin in naive lymphocyte adhesion to high endothelial venules in a mucosal site. *J. Immunol. 163:1382.*
16. Yanagita, M., T. Hiroi, N. Kitagaki, S. Hamada, H. O. Ito, H. Shimauchi, S. Murakami, H. Okada, and H. Kiyono. 1999. Nasopharyngeal-associated lymphoreticular tissue (NALT) immunity: fimbriae-specific Th1 and Th2 cell-regulated IgA responses for the inhibition of bacterial attachment to epithelial cells and subsequent inflammatory cytokine production. *J. Immunol. 162:3559.*
17. Elson, C. O. 1989. Cholera toxin and its subunits as potential oral adjuvants. *Curr. Top. Microbiol. Immunol. 146:29.*
18. Hiroi, T., M. Yanagita, H. Iijima, K. Iwatani, T. Yoshida, K. Takatsu, and H. Kiyono. 1999. Deficiency of IL-5 receptor α-chain selectively influences the development of the common mucosal immune system independent IgA-producing B-1 cell in mucosa-associated tissues. *J. Immunol. 162:821.*
19. Hiroi, T., M. Yanagita, N. Ohta, G. Sakaue, and H. Kiyono. 2000. IL-15 and IL-15 receptor selectively regulate differentiation of common mucosal immune system-independent B-1 cells for IgA responses. *J. Immunol. 165:4329.*
20. Stavnezer, J. 2000. Molecular processes that regulate class switching. *Curr. Top. Microbiol. Immunol. 245:127.*
21. Fukuyama, S., T. Hiroi, Y. Yokota, P. D. Rennert, M. Yanagita, N. Kinoshita, S. Terawaki, T. Shikina, M. Yamamoto, Y. Kurono, et al. 2002. Initiation of NALT organogenesis is independent of the IL-7R, LTβR, and NIK signaling pathways but requires the Id2 gene and CD3$^-$CD4$^+$CD45$^+$ cells. *Immunity 17:31.*

Intestinal γδ T Cells Develop in Mice Lacking Thymus, All Lymph Nodes, Peyer's Patches, and Isolated Lymphoid Follicles[1]

Satoshi Nonaka,* Tomoaki Naito,* Hao Chen,* Masafumi Yamamoto,‡ Kazuyo Moro,* Hiroshi Kiyono,† Hiromasa Hamada,* and Hiromichi Ishikawa[2]*

Through analysis of athymic (*nu/nu*) mice carrying a transgenic gene encoding GFP instead of RAG-2 product, it has recently been reported that, in the absence of thymopoiesis, mesenteric lymph nodes and Peyer's patches (PP) but not gut cryptopatches are pivotal birthplace of mature T cells such as the thymus-independent intestinal intraepithelial T cells (IEL). To explore and evaluate this important issue, we generated *nu/nu* mice lacking all lymph nodes (LN) and PP by administration of lymphotoxin-β receptor-Ig and TNF receptor 55-Ig fusion proteins into the timed pregnant *nu/+* mice that had been mated with male *nu/nu* mice (*nu/nu* LNP$^-$ mice). We also generated *nu/nu aly/aly* (*aly*, *alymphoplasia*) double-mutant mice that inherently lacked all LN, PP, and isolated lymphoid follicles. Although γδ-IEL were slightly smaller in number than those in *nu/nu* mice, substantial colonization of γδ-IEL was found to take place in the intestinal epithelia of *nu/nu* LNP$^-$ and *nu/nu aly/aly* mice. Notably, the population size of a major CD8αα$^+$ γδ-IEL subset was maintained, the use of TCR-γ-chain variable gene segments by these γδ-IEL was unaltered, and the development of cryptopatches remained intact in these *nu/nu* LNP$^-$ and *nu/nu aly/aly* mice. These findings indicate that all LN, including mesenteric LN, PP, and isolated lymphoid follicles, are not an absolute requirement for the development of γδ-IEL in athymic *nu/nu* mice. *The Journal of Immunology*, 2005, 174: 1906–1912.

Over the past 2 decades, it has been revealed that numerous intestinal intraepithelial T cells (IEL)[3] have cellular and behavioral characteristics distinct from those of thymus-derived peripheral T cells (1–8). In mice, IEL are enriched with TCR-γδ T cells (γδ-IEL) (9, 10), and virtually all γδ-IEL and many αβ-IEL, unlike thymus-derived CD8αβ T cells that use the ζ-chain as part of their CD3 complex, express the unique CD8αα homodimer (11–14) and can use the FcRγ-chain in place of the ζ-chain (15–17). Along these findings, growing evidence has indicated thymus-independent (TI) development of such CD8αα-expressing IEL (TI-IEL) (5, 7, 11, 12, 18). Detection of RAG-1 and RAG-2 transcripts (12, 19–22) and identification of a small number of T-lineage-committed TCR$^-$ lymphocytes in IEL from wild-type mice (2, 12, 19, 20, 23–25) supported the concept of localized development of IEL in the epithelial layer in situ. However, it should be pointed out that the original view of extrathymic generation of CD8αα$^+$ αβ-IEL is now inconsistent with the results of recent studies in which the thymus-dependent generation of every αβ-IEL, including the CD8αα-expressing subset, is unequivocally demonstrated (26, 27).

Our search (28) for anatomical sites of IEL generation revealed multiple tiny clusters filled with ~1000 c-Kit$^+$IL-7R$^+$Lin$^-$ (Lin, lineage markers) lymphohemopoietic cells in the lamina propria (LP) of the intestinal crypt (cryptopatches (CP)). Data obtained through a series of CP studies strongly indicated that CP were essential sites for the extrathymic development of precursor T cells destined to become TI-IEL (22, 28–30). Specifically, the presence of both TCR-γ and -β germline transcripts in the c-Kit$^+$IL-7R$^+$Lin$^-$ CP lymphocytes (30) has emphasized that various DNA recombination enzymes are able to approach these chromosomal segments to commence the region-specific recombinations (31–33). On the whole, these findings lend strong support to the idea that T lineage-committed precursors, which match the developmental stage of triple-negative c-Kit^{high}CD44$^+$CD25$^{low/-}$ thymocytes before pre-Tα gene transcription (34, 35), but after expression of CD3ε-specific mRNA (35, 36), are present in gut CP (30). One impediment to this conclusion has been the detection of a marginal level of RAG-2 transcripts for CP lymphocytes (22). However, the analysis of athymic (*nu/nu*), bone marrow (BM) chimeric mice revealed that the development of donor BM-derived TI-IEL proceeded through several consecutive steps (30). BM-derived TCR$^-$ IEL first appeared within villous epithelia overlying the regenerated CP filled with BM-derived c-Kit$^+$IL-7R$^+$Lin$^-$ cells. These TCR$^-$ IEL subsequently emerged throughout the epithelia, and thereafter, conversion of TCR$^-$ to TCR$^+$ IEL, the final

*Department of Microbiology and Immunology, Keio University School of Medicine, and †Division of Mucosal Immunology, Department of Microbiology and Immunology, Institute of Medical Science, University of Tokyo, Tokyo, Japan; and ‡Department of Oral Medicine, Nihon University School of Dentistry, Chiba, Japan

Received for publication August 9, 2004. Accepted for publication December 10, 2004

The costs of publication of this article were defrayed in part by the payment of page charges. This article must therefore be hereby marked *advertisement* in accordance with 18 U.S.C. Section 1734 solely to indicate this fact.

[1] This work was supported by Grant-in-Aid for Creative Scientific Research (13GS0015); the Japan Society for the Promotion of Science; a Grant-in-Aid for Scientific Research on Priority Areas A; a Grant-in-Aid for the 21st Century of Excellence Program entitled Understanding and Control of Life's Function via Systems Biology (Keio University); the Special Coordination Fund for Promoting Science and Technology, Ministry of Education, Culture, Sports, Science, and Technology; and Health Science Research Grants from the Ministry of Health, Labor, and Welfare.

[2] Address correspondence and reprint requests to Dr. Hiromichi Ishikawa, Department of Microbiology and Immunology, Keio University School of Medicine, Shinjuku-ku, Tokyo 160-8582, Japan. E-mail address: h-ishika@sc.itc.keio.ac.jp

[3] Abbreviations used in this paper: IEL, intestinal intraepithelial T cell; *aly*, alymphoplasia; BM, bone marrow; CP, cryptopatch; DN, double negative; iFABP, intestinal fatty acid-binding protein; IEC, intestinal epithelial cell; ILF, isolated lymphoid follicle; Lin, lineage marker; LNP$^-$, lymph node- and Peyer's patch deficient; LP, lamina propria; LT, lymphotoxin; LTβ-R, lymphotoxin-β receptor; MLN, mesenteric lymph node; PP, Peyer's patch; RORγt, retinoic acid-related orphan receptor; SCF, stem cell factor; Tg, transgenic; TI, thymus independent.

0022-1767/05/$02.00

step, took place very slowly. These results in conjunction with above-mentioned findings (2, 12, 19–25) have led us to conclude that TI-IEL complete their late maturational events, such as RAG-mediated TCR gene rearrangement, at a very slow rate in the epithelial layer in situ.

Recently, however, a new scenario for the extrathymic development of TI-IEL in *nu/nu* mice was described (37). By assessing RAG-2 expression in transgenic (Tg) *nu/nu* mice carrying a bacterial artificial chromosome encoding a GFP reporter instead of RAG-2, it was demonstrated that extrathymic T lymphopoiesis occurred mainly in mesenteric lymph nodes (MLN) and less in Peyer's patches (PP), but not in CP (37). To evaluate these new and important findings, we generated *nu/nu* mice that lacked all LN and PP by administration of lymphotoxin-β receptor (LTβ-R)-Ig and TNF-R55-Ig fusion proteins into pregnant *nu/+* mice (38) and double-mutant *nu/nu aly/aly* (*aly*, *alymphoplasia*) mice that lacked all LN, PP, as well as newly identified intestinal isolated lymphoid follicles (ILF) (39). We confirmed that these two kinds of mice harbored numerous $\gamma\delta$-IEL in the epithelial compartments of the small intestines and were found to retain gut CP. The significance of these findings is discussed from the viewpoint that all LN, PP, and ILF are dispensable anatomical sites for the generation of TI-IEL in the athymic *nu/nu* condition.

Materials and Methods

Mice

BALB/cA Jcl *nu/nu* (*nu/nu*), BALB/cA Jcl *nu/+* (*nu/+*), *aly/aly* Jcl mutant and C.B-17/Icr Jcl *scid/scid* (*scid/scid*) mice were purchased from CLEA Japan (Tokyo, Japan). TCR-$\gamma\delta$ (KN6)-Tg mice on the BALB/c background were described previously (40). Female KN6-Tg mice were crossed with *scid/scid* mice to generate KN6 *scid/+* mice, then they were backcrossed with *scid/scid* mice to obtain KN6 *scid/scid* mice. The presence of KN6-Tg was determined by PCR analysis of tail DNA with a set of primers to the KN6 Tg (5′-CAGATCCTTCCAGTTCATCC-3′ and 5′-CAGTCACTT GGGTTCCTTGTCC-3′), and the homozygous *scid/scid* genotype was determined by the absence of TCR-$\alpha\beta^+$ T cells in PBL. We generated transplacentally manipulated *nu/nu* and *nu/+* mice that lack all LN and PP according to essentially the same method described previously (38). In brief, timed-pregnant *nu/+* mice that had been mated with male *nu/nu* mice were i.v. injected with 200 μg of both LTβ-R-Ig and TNFR-55-Ig fusion proteins on gestational days 13 and 16. All mice used for experiments were between 8 and 18 wk of age, and absence of a thymus in various athymic mice was checked at necropsy. All animal procedures described in this study were performed in accordance with the guidelines for animal experiments of Keio University School of Medicine.

Production of nu/nu aly/aly *mice and genotyping of aly mutation*

Because *nu/nu* and *aly/aly* mothers are incapable of nursing the neonates, we used an in vitro fertilization technique (41) to produce (*nu/nu*×*aly/aly*)F_1 hybrid mice, then these heterozygous *nu/+ aly/+* mice were intercrossed to obtain *nu/nu aly/+*, *nu/nu aly/aly*, and *nu/+ aly/+ nu/+ aly/aly* littermates. To determine *aly/aly*, *aly/+*, and *+/+* alleles, the TaqMan assay of tail DNA was performed using the ABI PRISM 7000 sequence detection system (PerkinElmer) as previously described (42). The primer sequences for *aly* were 5′-GCCTACTGACATCCCGAGCTA-3′ (forward primer) and 5′-GCAGGACTGGGCTGGAAGA-3′ (reverse primer). The oligonucleotide probe corresponding mutant *aly* allele was 5′-AGACCG TACTGTTGAAG-3′ (FAM labeled), and the oligonucleotide probe corresponding wild-type allele was 5′-AGACCGTACCGTTGAA-3′ (VIC labeled). Underlining in sequences indicates point mutation. The 3′ end of each probe carried the quencher that suppressed the fluorescence of the reporter dyes. Each DNA sample was amplified with the TaqMan Universal master mixture containing AmpliTaq Gold DNA polymerase according to the manufacturer's instructions (Applied Biosystems). PCR conditions were 2 min at 50°C, 10 min at 95°C, 15 s at 95°C, and 1 min at 60°C for 40 cycles. During PCR, fluorescence developed when the oligonucleotide hybridized to perfectly matching DNA, and the exonuclease activity of *Taq* polymerase separated the quencher from the reporter dye. After PCR, the fluorescence yield for the two different dyes was measured and presented in a two-dimensional graph.

Antibodies

The following mAbs, described previously (22, 28–30, 39), were used. For immunohistochemical and immunofluorescence stainings: anti-$\gamma\delta$ (GL-3), anti-c-Kit (ACK-2), anti-B220 (RA3-6B2), and anti-IgA (C10-3) were used. For flow cytometric analysis, FITC-conjugated anti-$\alpha\beta$ (H57-597), anti-$\gamma\delta$ (GL-3), anti-Vγ1 (2.11; gift from Dr. S. Tonegawa, Center for Learning and Memory, MIT, Cambridge, MA), anti-Vγ4 (UC3-10A6), anti-Vγ7 (GL-1; gift from Dr. L. Lefrancois, Department of Medicine, Division of Immunology, University of Connecticut Health Center, Farmington, CT), anti-CD4 (GK 1.5), biotinylated anti-$\gamma\delta$ (GL-3), anti-B220 (RA3-6B2), anti-CD8α (53-6.7), and anti-c-kit (ACK-2), and PE-conjugated anti-CD8β (53-5.8) and anti-CD4 (GK 1.5) were used.

Immunohistochemical procedure

Longitudinally opened small intestine, ~10 mm in length, was pasted on a filter paper to form a horizontal section and then embedded in OCT compound (Tissue-Tek; Miles) at −80°C. The tissue segments were sectioned with a cryostat at 6 μm, and sections were preincubated with Block-Ace (Dainippon Pharmaceutical) to block nonspecific binding of mAbs. The sections were then incubated with hamster (anti-$\gamma\delta$) or rat (anti-c-Kit, anti-B220, or anti-IgA) mAb for 30 min at 37°C and rinsed three times with PBS, followed by incubation with biotin-conjugated goat anti-hamster IgG Ab (5 μg/ml; Cedarlane Laboratories) or with biotin-conjugated goat anti-rat IgG (5 μg/ml; Cedarlane Laboratories). Subsequently, the sections were washed three times with PBS, then incubated with avidin-biotin peroxidase complexes (Vectastain ABC kit; Vector Laboratories). Histochemical color development was achieved with Vectastain 3,3′-diaminobenzidine substrate kit (Vector Laboratories) according to the manufacturer's instructions. Finally, the sections were counterstained with hematoxylin for microscopy. Endogenous peroxidase activity was blocked with 0.3% H_2O_2 and 0.1% NaN_3 in distilled water for 10 min at room temperature. Tissue sections incubated with either nonimmune hamster serum or isotype-matched normal rat IgG showed only minimal background staining.

Immunofluorescence procedure

Tissue segments from thymus, spleen, inguinal LN, MLN, and PP from KN6 *scid/scid* mice were embedded in OCT compound at −80°C. The small intestine of KN6 *scid/scid* mice was longitudinally opened along the mesenteric wall, then intestine, ~10 mm in length, that had been rolled to form a vertical section was embedded in OCT compound at −80°C. Cryostat tissue sections, 6-μm thick, were fixed in acetone for 10 min at room temperature, washed three times with PBS, then pretreated with Block-Ace. Subsequently, the sections were incubated with anti-c-Kit mAb (ACK-2) for 60 min at 4°C, followed by incubation with PE-conjugated goat $F(ab')_2$ anti-rat IgG (H+L) (Invitrogen Life Technologies). The sections were then incubated with anti-$\gamma\delta$ mAb (GL-3) and counterstained with FITC-conjugated goat anti-hamster IgG (H+L) (Jackson ImmunoResearch Laboratories). Finally, the sections were examined under a fluorescence microscope (Axiovert 100; Carl Zeiss) equipped with an image analysis system (Signal Analytics).

Flow cytometry

IEL were isolated according to methods described previously (22). Lymphoid cells were incubated first with biotinylated mAb, then with streptavidin-PE (BD Biosciences) and FITC-conjugated second mAb. Stained cells were suspended in staining medium (Hanks' solution without phenol red, 0.02% NaN_3, and 2% heat-inactivated FBS) containing 0.5 μg/ml propidium iodide and analyzed using FACScan with CellQuest software (BD Biosciences). Dead cells were excluded by propidium iodide gating. Three-color analysis of IEL was also performed. IEL were incubated first with anti-CD8α mAb (biotinylated), then with streptavidin-Tri-Color (Caltag Laboratories). After washing, IEL were counterstained with two combinations of two PE-conjugated mAbs (anti-CD8β and anti-CD4 mAbs) and one FITC-conjugated mAb (anti-$\gamma\delta$), respectively. Lymphoid cells were incubated with anti-FcγR II/III mAb (2.4G2) before staining to block nonspecific binding of labeled mAbs to FcR.

Results

Development of $\gamma\delta$-IEL in nu/nu *mice is independent of all LN and PP*

To explore whether MLN are essential anatomical sites for the generation of TI-IEL in athymic *nu/nu* mice (37), we generated *nu/nu* mice that lacked all LN and PP. Pregnant *nu/+* female mice that had been mated with *nu/nu* male mice were injected with

LTβ-R-Ig and TNF-R55-Ig fusion proteins according to the protocol described by Rennert et al. (38), and the presence or the absence of LN and PP was determined in the progeny at 8 wk of age under a stereomicroscope. Although PP were absent from all treated mice, markedly attenuated remnants of MLN were present in about one-fifth of them. However, in every MLN-deficient *nu/nu* and *nu/+* offspring, the development of mandibular, axillary, inguinal, and popliteal (data not shown) LN (i.e., peripheral LN) and cervical (data not shown), iliac, and sacral LN (i.e., mucosal LN) was also ablated (LNP⁻ mice; Fig. 1).

Flow cytometric analysis of IEL isolated from *nu/nu*, *nu/nu* LNP⁻, *nu/+*, and *nu/+* LNP⁻ mice was performed using anti-TCR-αβ and anti-TCR-γδ mAbs. Consistent with well-established findings (3, 4, 8, 43), the proportion of αβ-IEL to γδ-IEL was sharply reduced, and the composition of IEL not expressing either type of TCR was expanded in athymic *nu/nu* conditions regardless of the presence or the absence of all LN and PP (Fig. 2*A*). In contrast, no significant differences in absolute numbers of IEL were observed between LNP⁻ and control LNP⁺ mice (data not shown). Notably, although the population size was slightly smaller by a factor of ~1.5 compared with that in IEL from control *nu/nu* mice, a large number of γδ-IEL was detected in IEL from *nu/nu* LNP⁻ mice (Fig. 2*A*). Compartmentalization of γδ-IEL within the epithelial layer of small intestine in *nu/nu* LNP⁻ mice was also verified by immunohistochemistry (Fig. 2*B*). These results indicate

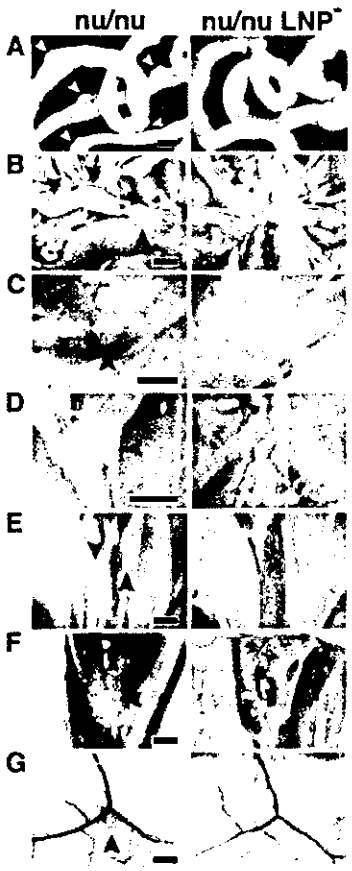

FIGURE 1. Development of PP and all LN in athymic *nu/nu* mice is ablated by in utero treatment with both LTβ-R-Ig and TNF-R55-Ig fusion proteins. PP (*A*), MLN (*B*), mandibular LN (*C*), axillary LN (*D*), iliac LN (*E*), sacral LN (*F*), and inguinal LN (*G*) are present in untreated *nu/nu* mice (arrowheads), but are undetectable in *nu/nu* mice that were treated in utero with both LTβ-R-Ig and TNF-R55-Ig fusion proteins (*nu/nu* LNP⁻ mice). Bar, 2 mm.

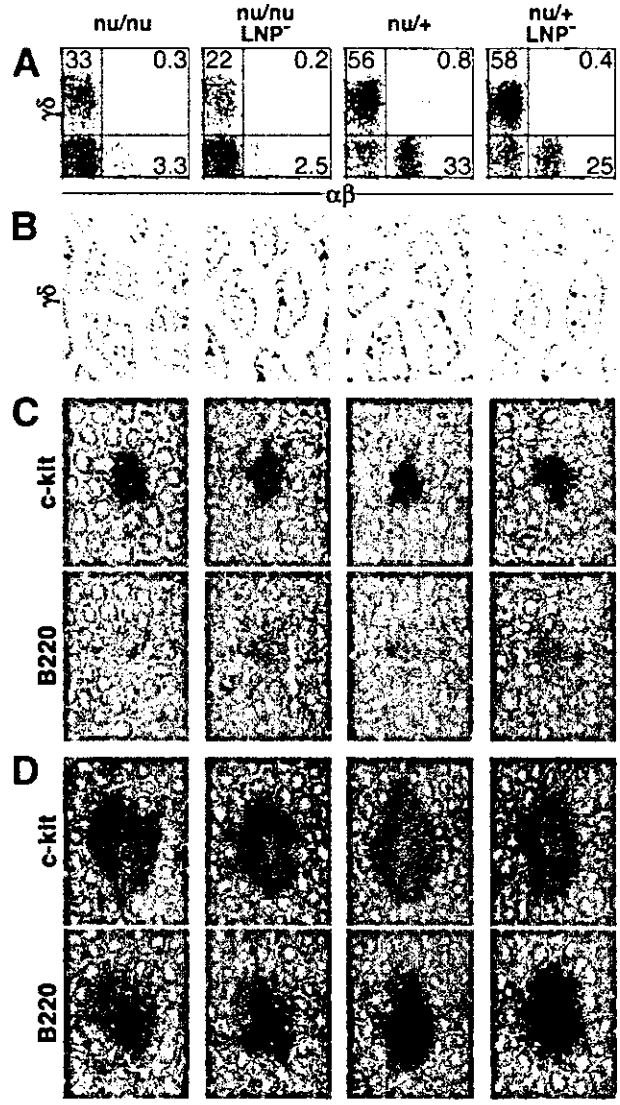

FIGURE 2. Flow cytometric analysis of IEL and immunohistochemical examination of small intestines from *nu/nu*, *nu/nu* LNP⁻, *nu/+*, and *nu/+* LNP⁻ mice. *A*, Although the population size of γδ-IEL in *nu/nu* LNP⁻ mice that lack all LN and PP is smaller than that of *nu/nu* mice, a substantial number of γδ-IEL are present in the epithelial compartment of *nu/nu* LNP⁻ mice, indicating that γδ-IEL are capable of developing in the absence of thymus, all LN including MLN, and PP. Note that the composition of αβ-IEL is reduced drastically in the athymic *nu/nu* condition compared with that in the euthymic *nu/+* condition. *B*, Representative immunohistochemical visualization of γδ-IEL in the small intestines of *nu/nu*, *nu/nu* LNP⁻, *nu/+*, and *nu/+* LNP⁻ mice (magnification, ×200). Although numbers of γδ-IEL in *nu/nu* LNP⁻ mice are decreased compared with those in *nu/nu* mice, colonization of γδ-IEL takes place in the absence of thymus, all LN including MLN, and PP (arrowheads). *C*, Representative immunohistochemical verification of CP in the small intestines of *nu/nu*, *nu/nu* LNP⁻, *nu/+*, and *nu/+* LNP⁻ mice (magnification, ×200). An average number and an approximate mass of CP filled with c-Kit⁺B200⁺ lymphocytes in these four different mice remain almost the same. *D*, Representative immunohistochemical verification of ILF in the small intestines of *nu/nu*, *nu/nu* LNP⁻, *nu/+*, and *nu/+* LNP⁻ mice (magnification, ×200). Note that a cluster of B220⁺ B cells that reside in the central region of ILF is surrounded by the layer of cells expressing c-Kit molecules.

that the development of γδ-IEL per se is independent of thymus, all LN, and PP.

With these findings in mind, we examined whether CP and ILF were present in these in utero manipulated LNP⁻ mice, because, in

contrast to PP that are already microscopically well developed just before birth (44), organogenesis of CP (28) and ILF (39) commences in early postnatal life. In fact, it was corroborated that the development of CP filled with closely packed c-Kit$^+$ lymphocytes (Fig. 2*C*) and ILF containing B220$^+$ B cell aggregation (Fig. 2*D*) remained intact in these *nu/nu* LNP$^-$ and *nu/+* LNP$^-$ mice.

Development of γδ-IEL in nu/nu aly/aly *double-mutant mice*

To ascertain the universality of the above findings, we explored the development of IEL in a mutant mouse that inherently lacked thymus, all LN, and PP, because fusion protein-treated LNP$^-$ mice might possess a minute and stereomicroscopically invisible MLN, even though this possibility appeared to be remote (38). With this purpose in mind, we generated *nu/nu aly/aly* double-mutant mice. In accordance with the earliest description (45), *nu/nu aly/aly* mice were devoid of all LN and PP (data not shown) as well as thymus. Importantly, substantial colonization of γδ-IEL in the small intestine of *nu/nu aly/aly* mice was verified by flow cytometric (Fig. 3*A*) and immunohistochemical (Fig. 3*B*) analyses. Furthermore, as inferred from our previous observations (28, 39), histogenesis of CP was detected (Fig. 3*C*), whereas development of ILF was completely blocked (Fig. 3*D*), in these double-mutant animals. Taking all of these results together (Figs. 2 and 3), neither thymus, all LN including MLN, PP, nor ILF is an absolute requirement for the development of γδ-IEL.

In this context, it is important to determine T and B cells and IgA$^+$ B cells that sojourn, respectively, in the spleen and LP of *nu/nu* LNP$^-$ and *nu/nu aly/aly* mice, because spleen is most likely the sole organized peripheral lymphoid tissue remaining in these animals, and *nu/nu aly/aly* mice lack intestinal IgA$^+$ B cell-producing plants such as PP and ILF. In contrast to abundant B220$^+$ B cells, mature T cells were virtually absent in the spleens of *nu/nu* LNP$^-$ (Fig. 4*A*) and *nu/nu aly/aly* (Fig. 4*C*) mice. In the small intestines, however, *nu/nu* LNP$^-$ mice possessed IgA$^+$ B cells (Fig. 4*B*), γδ-IEL, CP, and well-developed ILF (Fig. 2), whereas *nu/nu aly/aly* mice possessed γδ-IEL (Fig. 3, *A* and *B*) and CP (Fig. 3*C*), but lacked IgA$^+$ B cells (Fig. 4*C*) and ILF (Fig. 4*D*). These results indicate that all LN, including MLN, PP, and ILF, are not an absolute requirement for the generation of γδ-IEL in *nu/nu* mice and that the *aly* mutation interferes the formation of PP and ILF, resulting in the impaired development of IgA$^+$ B cells in villous LP.

Phenotypic and Vγ gene usage analyses of γδ-IEL in nu/nu *LNP*$^-$ *and* nu/nu aly/aly *mice*

The data reported to date indicate that γδ-IEL are potentially capable of developing in *nu/nu* mice lacking all LN, PP, and ILF. In this regard, however, it is reasonable to consider the possibility that γδ-IEL generated under such harsh conditions might differ from those generated in *nu/nu* mice possessing all LN, PP, and ILF. To address this issue, we conducted flow cytometric analysis of γδ-IEL isolated from *nu/nu*, *nu/nu* LNP$^-$, and *nu/nu aly/aly* mice. Although absolute numbers of γδ-IEL were lower by a factor of 2 compared with those in *nu/nu* mice (Fig. 5*A*), the composition of the major γδ-IEL subset expressing CD8αα homodimer (Fig. 5*A*) and the Vγ1, Vγ4, and Vγ7 gene segment used by such γδ-IEL (Fig. 5*B*) remained the same in both *nu/nu* LNP$^-$ and *nu/nu aly/aly* mice. Collectively, these results indicate that the absence of all LN, PP, and ILF exerts only a small effect on the phenotypic configuration of γδ-IEL in *nu/nu* mice.

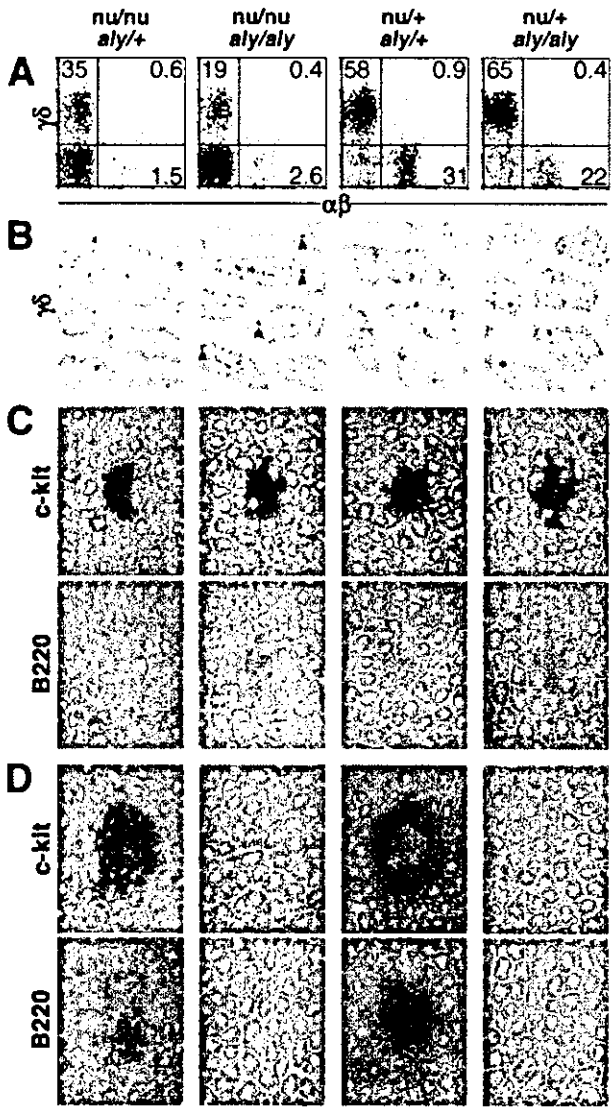

FIGURE 3. Flow cytometric analysis of IEL and immunohistochemical examination of small intestines from *nu/nu aly/+*, *nu/nu aly/aly*, *nu/+ aly/+*, and *nu/+ aly/aly* mice. *A*, Although the population size of γδ-IEL in *nu/nu aly/aly* mice that lack all LN, PP, and ILF is smaller than that in *nu/nu aly/+* mice, a significant number of γδ-IEL are present in the epithelial compartment of *nu/nu aly/aly* mice, indicating that γδ-IEL are capable of developing in the absence of thymus, all LN including MLN, PP, and ILF. Note that the composition of αβ-IEL is reduced drastically in the athymic *nu/nu* condition compared with that in the euthymic *nu/+* condition. *B*, Representative immunohistochemical verification of γδ-IEL in the small intestines of *nu/nu aly/+*, *nu/nu aly/aly*, *nu/+ aly/+*, and *nu/+ aly/aly* mice (magnification, ×200). Although numbers of γδ-IEL in *nu/nu aly/aly* mice are lower by a factor of 1.5–2 compared with those in *nu/nu aly/+* mice, a significant colonization of γδ-IEL takes place in the absence of thymus, all LN including MLN, PP, and ILF (arrowheads). *C*, Representative immunohistochemical verification of CP in the small intestines of *nu/nu aly/+*, *nu/nu aly/aly*, *nu/+ aly/+*, and *nu/+ aly/aly* mice (magnification, ×200). Although an average number of CP filled with c-Kit$^+$B220$^-$ lymphocytes in these four different mice remain almost the same, an approximate mass of CP present in *nu/nu aly/aly* and *nu/+ aly/aly* mice is slightly reduced compared with that of CP present in *nu/nu aly/+* and *nu/+ aly/+* mice. *D*, Representative immunohistochemical verification of ILF in the small intestines of *nu/nu aly/+*, *nu/nu aly/aly*, *nu/+ aly/+*, and *nu/+ aly/aly* mice (magnification, ×200). Note that ILF are undetectable throughout the small intestinal mucosa of *nu/nu aly/aly* and *nu/+ aly/aly* mice.

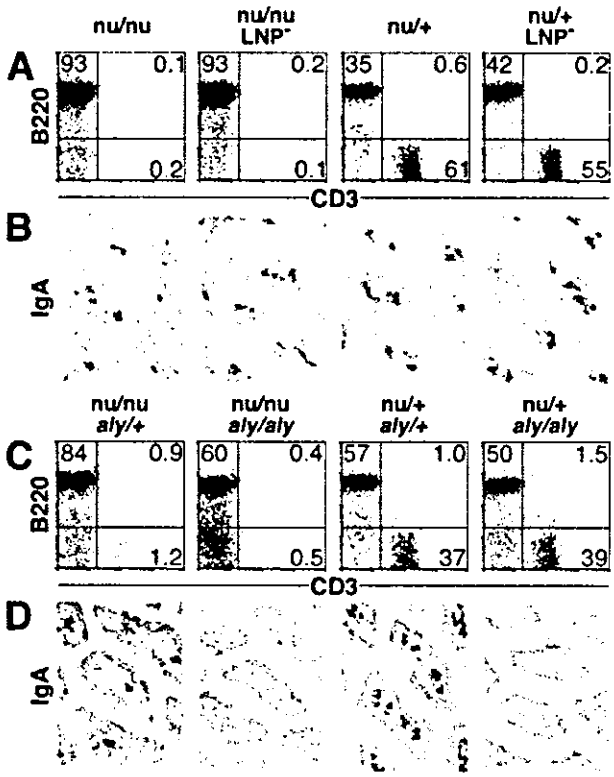

FIGURE 4. Flow cytometric analysis of splenic T and B cells and immunohistochemical verification of intestinal IgA⁺ B cells in *nu/nu*, *nu/nu* LNP⁻, *nu/nu aly/+*, and *nu/nu aly/aly* mice. *A*, Although mature CD3⁺ T cells are nearly absent from the spleens of *nu/nu* and *nu/nu* LNP⁻ mice, abundant B220⁺ B cells are detected in the spleens of these athymic animals. Colonization of IgA⁺ B cells in the villous LP of *nu/nu*, *nu/nu* LNP⁻, *nu/+*, and *nu/+* LNP⁻ mice is comparable. *B*, Only a marginal number of mature CD3⁺ T cells are detected in the spleens of *nu/nu aly/+* and *nu/nu aly/aly* mice, and a large fraction of the remaining lymphoid cells consists of B220⁺ B cells. In contrast, villous LP of *nu/nu aly/aly* and *nu/+ aly/aly* mice has no IgA⁺ B cells.

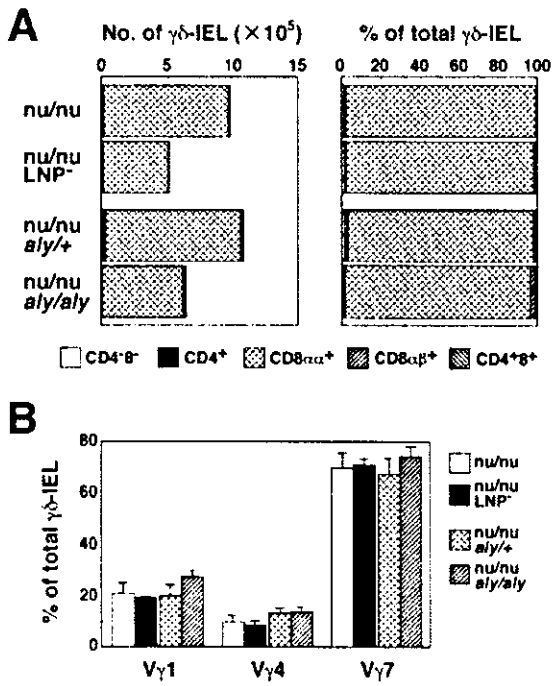

FIGURE 5. Flow cytometric analysis of γδ-IEL from *nu/nu*, *nu/nu* LNP⁻, nu/nu *aly/+*, and *nu/nu aly/aly* mice and Vγ gene segments used by γδ-IEL in these athymic *nu/nu* mice. *A*, Three-color analysis was performed. Absolute numbers of double-negative (CD4⁻8⁻), single-positive (CD4⁺, CD8αα⁺, or CD8αβ⁺), and double-positive (CD4⁺8⁺) subsets in the γδ-IEL population were calculated on the basis of total numbers of γδ-IEL. Data are the mean values from five mice per group. *B*, Two-color analysis was performed. IEL isolated from these *nu/nu* mice were incubated first with anti-TCR-γδ mAb (biotinylated), then with streptavidin-PE and FITC-conjugated anti-Vγ1, anti-Vγ4, or anti-Vγ7 mAb. The results are the mean ± SD of data obtained from four mice per group.

Development of c-Kit⁺ γδ-IEL in scid/scid *mice expressing Tg TCR-γδ*

We have shown that IL-7 produced by intestinal epithelial cells (IEC) is important for intraintestinal development of γδ-IEL and is crucial for organization of intestinal mucosal lymphoid tissues, such as PP and CP (18). It has also been shown that c-Kit and stem cell factor (SCF) are expressed by γδ-IEL and IEC, respectively, and signaling through c-Kit/SCF is indispensable for normal development of γδ-IEL (46, 47). Thus, these previous (46, 47) and the present findings in conjunction with results obtained with BM chimeric mice (30), reinforce the idea that the development of γδ-IEL takes place in the intestinal mucosa in situ. In an attempt to confirm and visualize directly the cellular events that proceed toward gut-oriented γδ-IEL generation, i.e., c-Kit⁺ CP cells→c-Kit⁺ TCR-γδ T cells→c-Kit⁻ γδ-IEL, we generated *scid/scid* mice expressing KN6-Tg TCR-γδ (48). Double-immunofluorescence analysis of small intestinal tissues containing CP highlighted these presumptive cellular events. Thus, a representative picture of jejunal tissue sections from KN6 *scid/scid* mice (Fig. 6*A*) shows that a cluster of c-Kit⁺ cells in a CP (red) does not express TCR-γδ, and that large numbers of γδ-IELs (green) are present in the epithelial layer, especially in the epithelium adjacent to CP. Notably, quite a large number of lymphocytes expressing both c-Kit and TCR-γδ molecules (yellow or orange) is also present in the epithelial and LP compartments of villi (Fig. 6*A*). Neither clustering c-Kit⁺ cells nor lymphocytes stained yellow/orange were detected in other lymphoid tissues, such as thymus, LN, PP, and spleen (data not shown). Flow cytometric analysis of cell surface c-Kit molecules on the gated γδ T cells confirmed that a large fraction of γδ-IEL was c-Kit positive, namely, double-positive TCR-γδ⁺c-Kit⁺ cells (Fig. 6*B*, *upper panel*). In contrast, abundant Tg γδ T cells residing in MLN, spleen, and thymus did not include such c-Kit-expressing, double-positive cells (Fig. 6*B*, *lower three panels*). Overall, these results support the above-described basic premise that the development of γδ-IEL takes place in the intestinal mucosa in situ. However, because KN6-Tg TCR-γδ-expressing cells have not been detected in the CP of KN6 *scid/scid* mice (Fig. 6*A*), whether CP are essential and indispensable anatomical sites in generating γδ-IEL remained highly contentious.

Discussion

Because most of the numerous lymphocytes residing in the murine IEC compartment unexpectedly turned out to be T cells (IEL), additional revelation toward the end of the last century indicated that they display phenotypic and functional characteristics distinct from those of other T cell populations and that their development does not necessarily depend on the thymus (TI-IEL) (1–18). Likewise, several lines of information have illuminated the distinctive T cell facets of human fetal intestine (49, 50), and on the basis of RAG expression, there may also be TI-IEL that develop in human (51, 52) and rat (53) intestines. Although evidence for the vestigial lymphocyte-producing function of gut mucosa is substantial, as mentioned above (2, 5, 7, 11, 12, 18–25, 49–53), recent studies

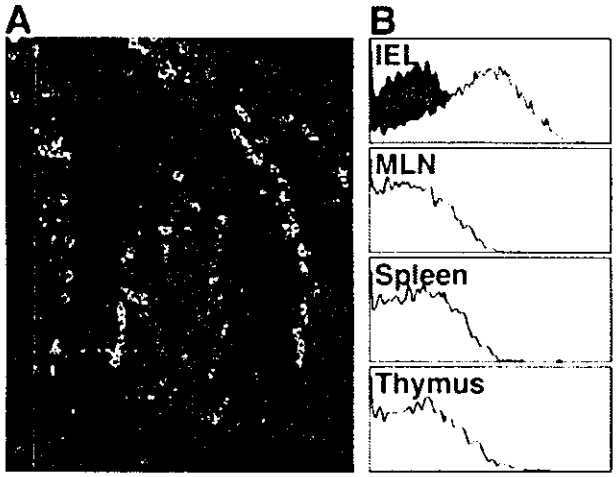

FIGURE 6. Double immunofluorescence analysis of small intestinal tissues containing CP and flow cytometric analysis of lymphocytes from KN6 *scid/scid* mice. *A*, Intestinal birthplace of intraepithelial γδ T cells (magnification, ×400). A cluster of lymphocytes in a CP is positively stained with anti-c-Kit mAb (PE), but not with anti-γδ mAb (FITC), resulting in a red color. Conversely, many IEL, especially those adjacent to CP, are positively stained with anti-γδ mAb (FITC), but not with anti-c-Kit mAb (PE), resulting in a green color. Note that a large number of lymphocytes present in the epithelial and LP compartments of villi are positively stained with anti-c-Kit mAb (PE) and anti-γδ mAb (FITC), resulting in a yellow or orange color. Neither the clusters filled with c-Kit$^+$ cells nor lymphocytes stained yellow or orange are detected in the other lymphoid organs, such as thymus, LN, and spleen. *B*, Expression of c-Kit molecules by Tg γδ T cells that colonize in the intestinal epithelial, MLN, and splenic and thymic compartments of KN6 *scid/scid* mice. IEL, MLN cells, spleen cells, and thymocytes were incubated first with anti-TCR-γδ mAb (biotinylated), then with streptavidin-PE and FITC-conjugated anti-c-Kit mAb. Profiles of c-Kit expression by the gated TCR-γδ$^+$ cell population are presented. The *dark area* in the *upper panel* depicts a FITC-positive cell profile of IEL that were stained simply with biotinylated anti-TCR-γδ mAb and streptavidin-PE (negative control). It is evident that IEL contain a large number of double-positive (TCR-γδ$^+$ c-Kit$^+$) cells, but that MLN, spleen, and thymus have no such double-positive cells.

have made it clear that CD8αα does not serve as a marker for TI development of αβ-IEL (26, 27). In contrast, because positive and/or negative selection of TCR-γδ T cells in the thymus is not as evident (26, 27), thymic dependency for functional TCR-γδ T cells is less obvious.

In an assessment of the expression of Tg-encoded GFP in place of RAG-2 protein, no evidence was obtained for a lymphopoietic process involving CP cells migrating into gut epithelium to undergo TCR gene rearrangement and maturation into αβ- and γδ-IEL even in the athymic *nu/nu* condition (37). Instead, MLN and, less efficiently, PP have been identified as the major extrathymic T cell-producing plants in athymic *nu/nu* mice, and the newly generated T cells migrate from MLN into thoracic duct lymph to reach the gut epithelia, indicating that MLN and PP are the pivotal sites in generating TI-IEL, mostly γδ-IEL (37). In this context, the development of γδ-IEL should be hampered in *nu/nu* mice that simultaneously lack MLN and PP. Our present findings argue against this scenario by showing that not only transplacentally manipulated *nu/nu* LNP$^-$ mice lacking all LN and PP, but also genetically defined *nu/nu aly/aly* mice lacking all LN, PP, and ILF harbor a substantial population of γδ-IEL (Fig. 2, *A* and *B*, and Fig. 3, *A* and *B*), although these two different mouse models may share the same confounding factors. In contrast to what was observed in *nu/nu* mice, the extrathymic pathway of IEL generation was shown to be totally repressed in the euthymic condition using the same GFP RAG-2 Tg mouse model (37). The authors proposed that all IEL, including CD8αα$^+$ IEL, in normal mice were the likely progeny of double-negative (DN) TCR-αβ$^+$ and -γδ$^+$ thymocytes and noted that extremely complex and unusual T cell characteristics of murine IEL with respect to their expression of various accessory, costimulation, activation, and adhesion markers (4, 5) might be brought about by the distinctive microenvironment of gut epithelium (37). In this context, for instance, many DN thymocytes somehow down-regulate cell surface expression of Thy-1 molecules, because a substantial fraction of IEL is Thy-1 negative, whereas most of them must up-regulate c-Kit molecules on the way to becoming IEL (46, 47) (Fig. 6). Even if all of those transfigurations (>20) are attributable to the inherent properties of gut epithelium, the biological significance as well as the molecular level of the mechanisms underlying such enigmatic cellular events remain highly contentious. It should also be pointed out that our recent findings (18) are inconsistent with this idea (37). γδ T cells are absent in IL-7$^{-/-}$ mice due to the selective blockade of TCR-γ gene rearrangements (54). Using the intestinal fatty acid-binding protein (iFABP) promoter, we reinstated the expression of IL-7 to mature IEC of IL-7$^{-/-}$ mice (iFABP-IL7) (18). Although γδ-IEL were restored in iFABP-IL7 mice as well as CP and PP, γδ T cells remained absent from all tissues, including thymus, spleen, and skin. These results clearly indicate that γδ-IEL generated in iFABP-IL7 mice are not of DN TCR-γδ$^+$ thymocyte origin and that the recombination of TCR-γ genes in TCR-precursor T cells takes place in situ with the assistance of IL-7 produced locally by IEC.

Our present findings provide compelling evidence for the development of γδ-IEL within the intestine of *nu/nu* mice that lack the thymus, all LN, PP, and ILF. It should be pointed out, however, that the population size and absolute numbers of γδ-IEL from *nu/nu* LNP$^-$ and *nu/nu aly/aly* mice are smaller than those from the corresponding control *nu/nu* mice (Figs. 2*A*, 3*A*, and 5*A*). These features would indicate that LN and PP, in fact, contribute to γδ-IEL numbers in the *nu/nu* condition. In contrast to the results obtained in GFP RAG-2 Tg mouse model (37), our previous RT-PCR analysis of lymphocytes from normal euthymic mice showed that under conditions in which mRNA from 50 thymocytes displayed a strong signal for RAG-2 transcripts and mRNA from 6250 RAG-2$^{-/-}$ thymocytes failed to display any detectable signals, very low levels of RAG-2 transcripts were constantly detected in an amount of mRNA equivalent to 6250 IEL and CP cells (22). These findings suggest that a small minority of IEL and possibly CP cells also is undergoing TCR gene rearrangement, that they are able to do so with a minimum amount of RAG-2 transcripts, or both. Actually, we still do not know how many RAG-1 and -2 molecules per nucleus are required to drive the region-specific V(D)J recombinations of TCR genes. It is possible that the amount of mRNA encoding RAG-1 and -2 molecules required by thymocytes for the successful recombination of TCR genes may not be that large. It should also be pointed out that using cell fate mapping, almost all αβ-IEL have recently been shown to be the progeny of immature CD4$^+$CD8$^+$ thymocytes (55). Furthermore, by using elegant and sophisticated approaches (55), it has been revealed that the retinoic acid-related orphan receptors (RORγt) detected in fetal lymphoid tissue-inducer cells are also expressed in cells within gut CP, and that γδ-IEL are not the progeny of such RORγt-positive CP lymphocytes. Specifically, however, it has remained an open question whether a small, but significant, fraction of lymphocytes in CP does not retain RORγt molecules or whether almost all CP lymphocytes express RORγt (55). In any event, to substantiate the intraintestinal development of γδ-IEL in these *nu/nu* LNP$^-$ and *nu/nu aly/aly* mice, clear identification of T cells

undergoing TCR gene rearrangement in the gut mucosa appears to be of critical importance.

Acknowledgments

We are grateful to Dr. L. Lefrancois for his critical reading of the manuscript. We thank N. Hosaka and M. Mori for their excellent technical assistance.

References

1. Rocha, B., D. Guy-Grand, and P. Vassalli. 1995. Extrathymic T cell differentiation. *Curr. Opin. Immunol. 7:235.*
2. Mowat, A. M., and J. L. Viney. 1997. The anatomical basis of intestinal immunity. *Immunol. Rev. 156:145.*
3. Klein, J. R. 1998. Thymus-independent development of gut T cells. *Chem. Immunol. 71:88.*
4. Lefrancois, L., and L. Puddington. 1999. Basic aspects of intraepithelial lymphocyte immunobiology. In *Mucosal Immunology.* P. L. Ogra, J. Mestecky, M. E. Lamm, W. Strober, J. Bienenstock, and J. R. McGhee, eds. Academic Press, San Diego, p. 413.
5. Aranda, R., B. C. Sydora, and M. Kronenberg. 1999. Intraepithelial lymphocytes: function. In *Mucosal Immunology.* P. L. Ogra, J. Mestecky, M. E. Lamm, W. Strober, J. Bienenstock, and J. R. McGhee, eds. Academic Press, San Diego, p. 429.
6. Poussier, P., and M. Julius. 1999. Speculation on the lineage relationships among $CD4^-8^+$ gut-derived T cells and their role(s). *Semin. Immunol. 11:293.*
7. Hayday, A., E. Theodoridis, E. Ramsburg, and J. Shires. 2001. Intraepithelial lymphocytes: exploring the Third Way in immunology. *Nat. Immunol. 2:997.*
8. Guy-Grand, D., and P. Vassalli. 2002. Gut intraepithelial lymphocyte development. *Curr. Opin. Immunol. 14:255.*
9. Goodman, T., and L. Lefrancois. 1988. Expression of the γ-δ T-cell receptor on intestinal $CD8^+$ intraepithelial lymphocytes. *Nature 333:855.*
10. Bonneville, M., C. A. Janeway, K. Ito, W. Haser, I. Ishida, N. Nakanishi, and S. Tonegawa. 1988. Intestinal intraepithelial lymphocytes are a distinct set of γδ T-cells. *Nature 336:479.*
11. Lefrancois, L. 1991. Phenotype complexity of intraepithelial lymphocyte of the small intestine. *J. Immunol. 147:1746.*
12. Guy-Grand, D., N. Cerf-Bensussan, B. Malissen, M. Malassis-Seris, C. Briottet, and P. Vassalli. 1991. Two gut intraepithelial $CD8^+$ lymphocyte populations with different T cell receptors: a role for the gut epithelium in T cell differentiation. *J. Exp. Med. 173:471*
13. Maloy, K. J., A. M. Mowat, R. Zamoyska, and I. N. Crispe. 1991. Phenotypic heterogeneity of intraepithelial T lymphocytes from mouse small intestine. *Immunology 72:555.*
14. Kawaguchi, M., M. Nanno, Y. Umesaki, S. Matsumoto, Y. Okada, Z. Cai, T. Shimamura, Y. Matsuoka, M. Ohwaki, and H. Ishikawa. 1993. Cytolytic activity of intestinal intraepithelial lymphocytes in germ-free mice is strain dependent and determined by T cells expressing γδ T-cell antigen receptors. *Proc. Natl. Acad. Sci. USA 90:8591.*
15. Malissen, M., A. Gillet, B. Rocha, J. Trucy, E. Vivier, C. Boyer, F. Kontgen, N. Brun, G. Mazza, E. Spanopoulou, et al. 1993. T cell development in mice lacking CD3-ζ/η gene. *EMBO J. 12:4347.*
16. Ohno, H., T. Aoe, S. Taki, D. Kitamura, Y. Ishida, K. Rajewsky, and T. Saito. 1993. Development and functional impairment of T cells in mice lacking CD3ζ chains. *EMBO J. 12:4357.*
17. Liu, C-P., R. Ueda, J. She, J. Sancho, B. Wang, G. Weddell, J. Loring, C. Kurahara, E. C. Dudley, A. Hayday, et al. 1993. Abnormal T cell development in $CD3\zeta^{-/-}$ mutant mice and identification of a novel T cell population in the intestine. *EMBO J. 12:4863.*
18. Laky, K., L. Lefrancois, E. G. Lingenheld, H. Ishikawa, J. M. Lewis, S. Olson, K. Suzuki, R. E. Tigelaar, and L. Puddington. 2000. Enterocyte expression of IL-7 induces development of γδ T cells and Peyer's patches. *J. Exp. Med. 191:1569.*
19. Guy-Grand, D., C. V. Broecke, C. Briottet, M. Malassis-Seris, F. Selz, and P. Vassalli. 1992. Different expression of the recombination activity gene RAG-1 in various populations of thymocytes, peripheral T cells and gut thymus-independent intraepithelial lymphocytes suggests two pathways of T cell receptor rearrangement. *Eur. J. Immunol. 22:505.*
20. Lin, T., G. Matsuzaki, H. Yoshida, N. Kobayashi, H. Kenai, K. Omoto, and K. Nomoto. 1994. $CD3^-CD8^+$ intestinal intraepithelial lymphocytes (IEL) and the extrathymic development of IEL. *Eur. J. Immunol. 24:1080.*
21. Boll, G., A. Rudolphi, S. Spieb, and J. Reimann. 1995. Regional specialization of intraepithelial T cells in the murine small and large intestine. *Scand. J. Immunol. 41:103.*
22. Oida, T., K. Suzuki, M. Nanno, Y. Kanamori, H. Saito, E. Kubota, S. Kato, M. Itoh, S. Kaminogawa, and H. Ishikawa. 2000. Role of gut cryptopatches in early extrathymic maturation of intestinal intraepithelial T cells. *J. Immunol. 164:3616.*
23. Hamad, M., M. Whetsell, J. Wang, and J. R. Klein. 1997. T cell progenitors in the murine small intestine. *Dev. Comp. Immunol. 21:435.*
24. Page, S. T., L. Y. Bogatzki, J. A. Hamerman, C. H. Sweenie, P. J. Hogarth, M. Malissen, R. M. Perlmutter, and A. M. Pullen. 1998. Intestinal intraepithelial lymphocytes include precursors committed to the T cell receptor αβ lineage. *Proc. Natl. Acad. Sci. USA 95:9459.*
25. Woodward, J., and E. Jenkinson. 2001. Identification and characterization of lymphoid precursors in the murine intestinal epithelium. *Eur. J. Immunol. 31:3329.*
26. Leishman, A. J., L. Gapin, M. Capone, E. Palmer, H. R. MacDonald, M. Kronenberg, and H. Cheroutre. 2002. Precursors of functional MHC class I- or class II-restricted $CD8\alpha\alpha^+$ T cells are positively selected in the thymus by agonist self-peptides. *Immunity 16:355.*
27. Cheroutre, H. 2004. Starting at the beginning: new perspectives on the biology of mucosal T cells. *Annu. Rev. Immunol. 22:217.*
28. Kanamori, Y., K. Ishimaru, M. Nanno, K. Maki, K. Ikuta, H. Nariuchi, and H. Ishikawa. 1996. Identification of novel lymphoid tissues in murine intestinal mucosa where clusters of $c\text{-}kit^+$ IL-$7R^+$ $Thy1^+$ lympho-hemopoietic progenitors develop. *J. Exp. Med. 184:1449.*
29. Saito, H., Y. Kanamori, T. Takemori, H. Nariuchi, E. Kubota, H. Takahashi-Iwanaga, T. Iwanaga, and H. Ishikawa. 1998. Generation of intestinal T cells from progenitors residing in gut cryptopatches. *Science 280:275.*
30. Suzuki, K., T. Oida, H. Hamada, O. Hitotsumatsu, M. Watanabe, T. Hibi, H. Yamamoto, E. Kubota, S. Kaminogawa, and H. Ishikawa. 2000. Gut cryptopatches: direct evidence of extrathymic anatomical sites for intestinal T lymphopoiesis. *Immunity 13:691.*
31. Alt, F. W., T. K. Blackwell, and G. D. Yancopoulos. 1987. Development of the primary antibody repertoire. *Science 238:1079.*
32. Hempel, W. M., I. Leduc, N. Mathieu, R. K. Tripathi, and P. Ferrier. 1998. Accessibility control of V(D)J recombination: lessons from gene targeting. *Adv. Immunol. 69:309.*
33. Ye, S.-K., K. Maki, T. Kitamura, S. Sunaga, K. Akashi, J. Domen, I. L. Weissman, T. Honjo, and K. Ikuta. 1999. Induction of germline transcription in the TCRγ locus by Stat5: implications for accessibility control by the IL-7 receptor. *Immunity 11:213.*
34. Saint-Ruf, C., K. Ungewiss, M. Groettrup, L. Bruno, H. J. Fehling, and H. von Boehmer. 1994. Analysis and expression of a cloned pre-T cell receptor gene. *Science 266:1208.*
35. Wilson, A., and H. R. MacDonald. 1995. Expression of genes encoding the pre-TCR and CD3 complex during thymus development. *Int. Immunol. 7:1659.*
36. Wang, B., N. Wang, C. E. Whitehurst, J. She, J. Chen, and C. Terhorst. 1999. T lymphocyte development in the absence of CD3ε or CD3γδε*ζ*. *J. Immunol. 162:88.*
37. Guy-Grand, D., O. Azogui, S. Celli, S. Darche, M. C. Nussenzweig, P. Kourilsky, and P. Vassalli. 2003. Extrathymic T cell lymphopoiesis: ontogeny and contribution to gut intraepithelial lymphocytes in athymic and euthymic mice. *J. Exp. Med. 197:333.*
38. Rennert, P. D., D. James, F. Mackay, J. L. Browning, and P. S. Hochman. 1998. Lymph node genesis is induced by signaling through the lymphotoxin β receptor. *Immunity 9:71.*
39. Hamada, H., T. Hiroi, Y. Nishiyama, H. Takahashi, Y. Masunaga, S. Hachimura, S. Kaminogawa, H. Takahashi-Iwanaga, T. Iwanaga, H. Kiyono, et al. 2002. Identification of multiple isolated lymphoid follicles on the antimesenteric wall of the mouse small intestine. *J. Immunol. 168:57.*
40. Kawaguchi-Miyashita, M., S. Shimada, H. Kurosu, N. Kato-Nagaoka, Y. Matsuoka, M. Ohwaki, H. Ishikawa, and M. Nanno. 2001. An accessory role of TCR-$\gamma\delta^+$ cells in the exacerbation of inflammatory bowel disease in TCRα mutant mice. *Eur. J. Immunol. 31:980.*
41. Hogan, B., F. Costantini, and E. Lacy. 1986. Recovery, culture, and transfer of embryo. In *Manipulating the Mouse Embryo.* B. Hogan, F. Costantini, and E. Lacy, eds. Cold Spring Harbor Laboratory, Plainview, p. 90.
42. Ranade, K., M.-S. Chang, C.-T. Ting, D. Pei, C.-F. Hsiao, M. Olivier, R. Pesich, J. Hebert, Y.-D. Chen, V. J. Dzau, et al. 2001. High-throughput genotyping with single nucleotide polymorphisms. *Genome Res. 11:1262.*
43. Lefrancois, L., and S. Olson. 1997. Reconstitution of the extrathymic intestinal T cell compartment in the absence of irradiation. *J. Immunol. 159:538.*
44. Yoshida, H., K. Honda, R. Shinkura, S. Adachi, S. Nishikawa, K. Maki, K. Ikuta, and S.-I. Nishikawa. 1999. IL-7 receptor α^+ $CD3^-$ cells in the embryonic intestine induces the organizing center of Peyer's patches. *Int. Immunol. 11:643.*
45. Miyawaki, S., Y. Nakamura, H. Suzuka, M. Koba, R. Yasumizu, S. Ikehara, and Y. Shibata. 1994. A new mutation, aly, that induces a generalized lack of lymph nodes accompanied by immunodeficiency in mice. *Eur. J. Immunol. 24:429.*
46. Puddington, L., S. Olson, and L. Lefrancois. 1994. Interactions between stem cell factor and c-Kit are required for intestinal immune system homeostasis. *Immunity 1:733*
47. Laky, K., L. Lefrancois, and L. Puddington. 1997. Age-dependent intestinal lymphoproliferative disorder due to stem cell factor deficiency. Parameters in small and large intestine. *J. Immunol. 158:1417.*
48. Ishida, I., S. Verbeek, M. Bonneville, S. Itohara, A. Berns, and S. Tonegawa. 1990. T cell receptor γδ and γ transgenic mice suggest a role of a γ gene silencer in the generation of αβ T cells. *Proc. Natl. Acad. Sci. USA 87:3067.*
49. Koningsberger, J. C., A. Chott, T. Logtenberg, L. J. Wiegman, R. S. Blumberg, G. P. van Berge Henegouwen, and S. P. Balk. 1997. TCR expression in human fetal intestine and identification of an early T cell receptor β-chain transcript. *J. Immunol. 159:1775.*
50. Howie, D., J. Spencer, D. DeLord, C. Pitzalis, N. C. Wathen, A. Dogan, A. Akbar, and T. T. MacDonald. 1998. Extrathymic T cell differentiation in the human intestine early in life. *J. Immunol. 161:5862.*
51. Lundqvist, C., V. Baranov, S. Hammarstrom, L. Athlin, and M.-L. Hammarstrom. 1995. Intra-epithelial lymphocytes: evidence for regional specialization and extrathymic T cell maturation in the human gut epithelium. *Int. Immunol. 7:1473.*
52. Lynch, S., D. Kelleher, R. McManus, and C. O'Farrelly. 1995. RAG1 and RAG2 expression in human intestinal epithelium: evidence of extrathymic T cell differentiation. *Eur. J. Immunol. 25:1143.*
53. Ramanathan, S., L. Marandi, and P. Poussier. 2002. Evidence for the extrathymic origin of intestinal TCR $\gamma\delta^+$ T cells in normal rats and for an impairment of this differentiation pathway in BB rats. *J. Immunol. 168:2182.*
54. Maki, K., S. Sunaga, and K. Ikuta. 1996. The V-J recombination of T cell receptor-γ genes is blocked in interleukin-7 receptor-deficient mice. *J. Exp. Med. 184:2423.*
55. Eberl, G., and D. R. Littman. 2004. Thymic origin of intestinal αβ T cells revealed by fate mapping of $ROR\gamma t^+$ cells. *Science 305:248.*

29. Inohara, N. & Nunez, G. NODs: intracellular proteins involved in inflammation and apoptosis. *Nature Rev. Immunol.* **3**, 371–382 (2003).
30. Rueffi-Brasse, A. A., Lee, W. P., Hurst, S. & Dixit, V. M. Rip2 participates in Bcl10 signaling and T-cell receptor-mediated NF-κB activation. *J. Biol. Chem.* **279**, 1570–1574 (2004).

Supplementary Information accompanies the paper on **www.nature.com/nature.**

Acknowledgements We thank D. Dornan and other members of the Dixit laboratory for discussions, E. Humke for help with illustrations, and K. O'Rourke, D. Wadley, Z. Gu, C. Olsson, M. Bauer, L. Tom, J. Kloss, M. Fuentes, M. Osborn, C. Tan, J. Hongo, T. Wong and A. Chuntharapai for technical assistance.

Competing interests statement The authors declare that they have no competing financial interests.

Correspondence and requests for materials should be addressed to V.M.D. (dixit@gene.com).

Regulation of Toll/IL-1-receptor-mediated gene expression by the inducible nuclear protein IκBζ

Masahiro Yamamoto[1], Soh Yamazaki[3], Satoshi Uematsu[1], Shintaro Sato[1,2], Hiroaki Hemmi[1], Katsuaki Hoshino[6], Tsuneyasu Kaisho[6], Hirotaka Kuwata[1], Osamu Takeuchi[1,2], Koichiro Takeshige[3], Tatsuya Saitoh[7], Shoji Yamaoka[7], Naoki Yamamoto[7], Shunsuke Yamamoto[8], Tatsushi Muta[3,4], Kiyoshi Takeda[5] & Shizuo Akira[1,2]

[1]*Department of Host Defense, Research Institute for Microbial Diseases, Osaka University,* [2]*ERATO, Japan Science and Technology Agency, 3-1 Yamada-oka, Suita Osaka 565-0871, Japan*
[3]*Department of Molecular and Cellular Biochemistry, Graduate School of Medical Sciences,* [4]*PRESTO, Japan Science and Technology Agency,* [5]*Department of Embryonic and Genetic Engineering, Medical Institute of Bioregulation, Kyushu University, 3-1-1 Maidashi, Higashi-ku, Fukuoka 812-8582, Japan*
[6]*RIKEN Research Center for Allergy and Immunology, 1-7-22 Suehiro-cho, Tsurumi-ku, Yokohama, Kanagawa 230-0045, Japan*
[7]*Department of Molecular Virology, Graduate School of Medicine, Tokyo Medical and Dental University, 1-5-45 Yushima, Bunkyo-ku, Tokyo 113-8519, Japan*
[8]*Department of Food and Nutrition, Beppu University, Kita-ishigaki, Beppu, Oita 874-0851, Japan*

Toll-like receptors (TLRs) recognize microbial components and trigger the inflammatory and immune responses against pathogens. IκBζ (also known as MAIL and INAP) is an ankyrin-repeat-containing nuclear protein that is highly homologous to the IκB family member Bcl-3 (refs 1–6). Transcription of IκBζ is rapidly induced by stimulation with TLR ligands and interleukin-1 (IL-1). Here we show that IκBζ is indispensable for the expression of a subset of genes activated in TLR/IL-1R signalling pathways. IκBζ-deficient cells show severe impairment of IL-6 production in response to a variety of TLR ligands as well as IL-1, but not in response to tumour-necrosis factor-α. Endogenous IκBζ specifically associates with the p50 subunit of NF-κB, and is recruited to the NF-κB binding site of the IL-6 promoter on stimulation. Moreover, NF-κB1/p50-deficient mice show responses to TLR/IL-1R ligands similar to those of IκBζ-deficient mice. Endotoxin-induced expression of other genes such as *Il12b* and *Csf2* is also abrogated in IκBζ-deficient macrophages. Given that the lipopolysaccharide-induced transcription of IκBζ occurs earlier than transcription of these genes, some TLR/IL-1R-mediated responses may be regulated in a gene expression process of at least two steps that requires inducible IκBζ.

IκBζ is thought to be induced in response to IL-1 or lipopolysaccharide (LPS) (TLR4 ligand)[4–6]. In addition to IL-1 and LPS, IκBζ messenger RNA was strongly upregulated on stimulation with peptidoglycan (PGN) (TLR2 ligand), bacterial lipoprotein (BLP) (TLR1/TLR2), flagellin (TLR5), MALP-2 (TLR6/TLR2), R-848 (TLR7) and CpG DNA (TLR9), but not with tumour-necrosis factor-α (TNF-α) (Fig. 1a). In contrast, other IκB family members such as IκBα and Bcl-3 were induced in response to TNF-α as well as the TLR ligands and IL-1. Thus, IκBζ is induced in the TLR/IL-1R signalling pathway but not the TNF signalling pathway. Furthermore, IL-1- or LPS-induced expression of IκBζ was completely abolished in *MyD88*$^{-/-}$ embryonic fibroblasts (MEFs; Fig. 1b), showing that IκBζ is inducible in the MyD88-dependent part of the TLR/IL-1R signalling pathway[7–15].

To elucidate the physiological role of IκBζ in the TLR/IL-1R response, we generated *IκBζ*$^{-/-}$ mice by targeted gene disruption (see Supplementary Discussion 1 and Supplementary Fig. 1a–d). *IκBζ*$^{-/-}$ splenocytes showed defective proliferation in response to LPS but not to anti-CD40, IL-4 and anti-IgM (Supplementary Fig. 1e, f), suggesting that the TLR4 response is impaired in *IκBζ*$^{-/-}$ cells. Moreover, although *IκBζ*$^{-/-}$ mice grew normally after birth, some of them started to develop atopic dermatitis-like skin lesions with acanthosis and lichenoid changes at the age of 4–5 weeks (Supplementary Fig. 2a, b). All *IκBζ*$^{-/-}$ mice developed the disease by the age of 10 weeks. Histological analysis of 5-week-old *IκBζ*$^{-/-}$ mice showed pathological changes in the conjunctiva, including a heavy lymphocyte infiltration into the submucosa and loss of goblet cells in the conjunctival epithelium (Supplementary Fig. 2c–f).

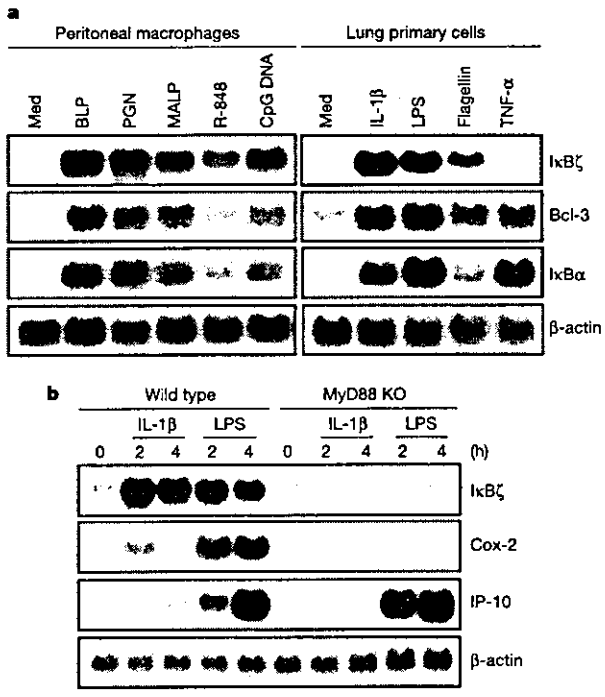

Figure 1 Specific induction of IκBζ on stimulation by TLR/IL-1R ligands. **a**, The indicated cells were stimulated with 100 ng ml^{-1} BLP, 10 μg ml^{-1} PGN, 30 ng ml^{-1} MALP-2, 100 nM R-848, 3 μM CpG DNA, 10 ng ml^{-1} IL-1β, 10 μg ml^{-1} LPS, 100 ng ml^{-1} flagellin and 10 ng ml^{-1} TNF-α for 2 h. Total RNA (10 μg) was extracted and subjected to northern blot analysis for expression of IκBζ, Bcl-3, IκBα and β-actin. Med, medium. **b**, *MyD88*$^{+/+}$ (wild type) and *MyD88*$^{-/-}$ (KO) MEFs were stimulated with 10 ng ml^{-1} IL-1β and 10 μg ml^{-1} LPS for the indicated periods. Total RNA (10 μg) was extracted and subjected to northern blot analysis for expression of IκBζ, Cox-2, IP-10 and β-actin.

We analysed the LPS-induced production of inflammatory mediators in macrophages. $I\kappa B\zeta^{+/+}$ macrophages produced TNF-α, IL-6 and nitric oxide (NO) in response to LPS (Fig. 2a). Although LPS-induced production of TNF-α and NO was normal, production of IL-6 was severely impaired in $I\kappa B\zeta^{-/-}$ macrophages. In addition, production of IL-6 via stimulation by various TLR ligands was also profoundly inhibited in $I\kappa B\zeta^{-/-}$ cells (Fig. 2b–d). Moreover, $I\kappa B\zeta^{-/-}$ cells exhibited defective IL-1-induced IL-6 production; however, IL-1-induced activation of NF-κB and mitogen-activated protein kinases was not impaired in these cells, indicating that there is no defect in the intracellular signalling pathways (Supplementary Fig. 3a, b). On the other hand, TNF-α-induced IL-6 production was not impaired in $I\kappa B\zeta^{-/-}$ cells (Fig. 2e). The impaired production of IL-6 in response to LPS correlated well with the reduced induction of IL-6 mRNA in $I\kappa B\zeta^{-/-}$ cells (Fig. 2f).

When full-length or a deletion mutant form of IκBζ was transfected into MEFs, full-length IκBζ, but not the deletion mutant, rescued the defective production of IL-6 on stimulation with IL-1 in $I\kappa B\zeta^{-/-}$ cells (Fig. 2g), suggesting that expression of IκBζ is required for TLR/IL-1-mediated production of IL-6. As the genes for IκBζ and IL-6 are inducible in response to TLR ligands and IL-1 (refs 4–6, 16, 17), we compared the time course of mRNA expression in macrophages. On stimulation with LPS, induction of IκBζ expression was observed at 30 min and reached maximal levels after 120 min. On the other hand, induction of IL-6 mRNA occurred at later time points compared with IκBζ or TNF-α (Fig. 2h). Taken together, these results indicate that the TLR/IL-1R-mediated expression of the IL-6 gene (*Il6*) requires the preceding induction of IκBζ. Given that IκBζ is also an inducible protein in TLR/IL-1R-mediated signalling pathways, the TLR/IL-1R-mediated production of pro-inflammatory IL-6 may be controlled in at least a two-step fashion.

Our data and those of a previous study[5] indicate the positive role of IκBζ in the TLR/IL-1R-mediated expression of IL-6. To test

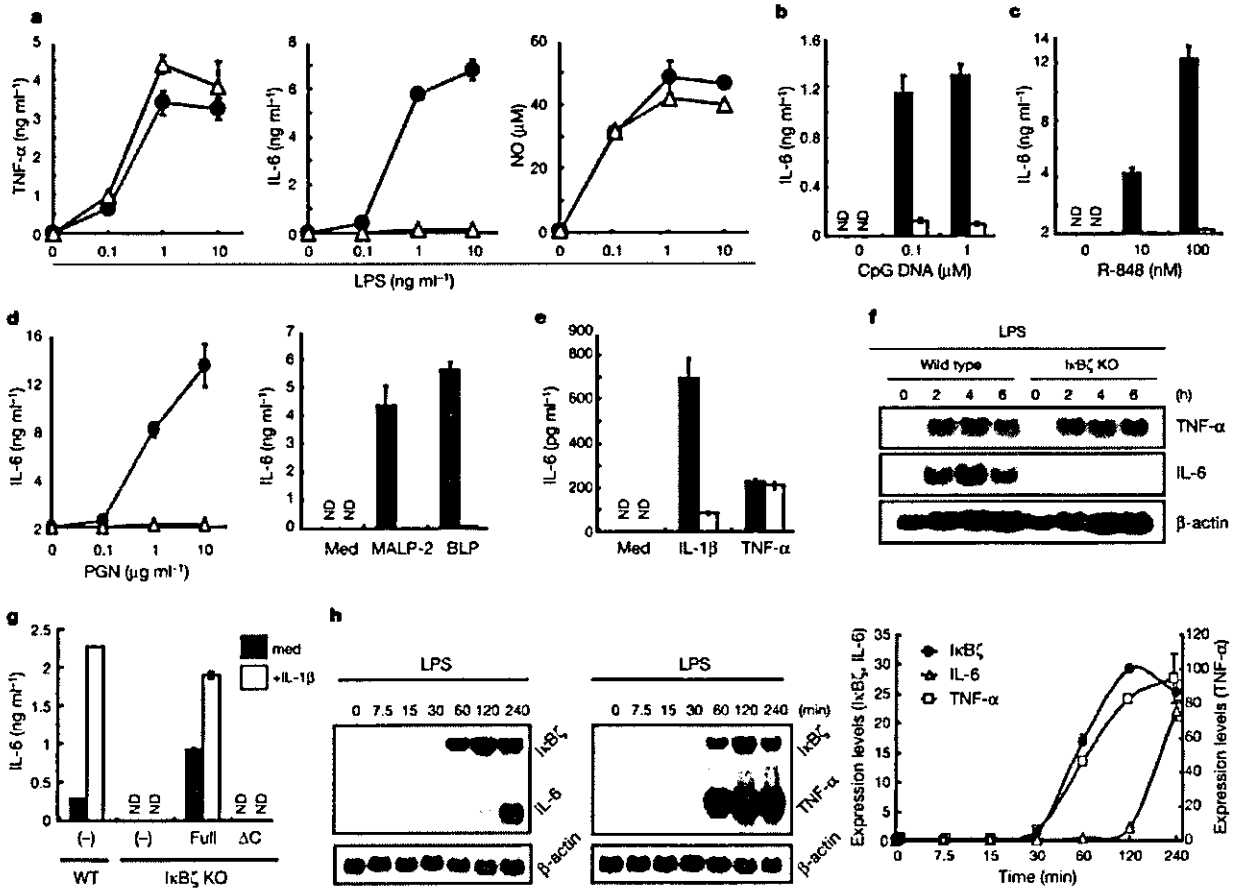

Figure 2 Immune responses in $I\kappa B\zeta^{-/-}$ cells and kinetics of IκBζ induction. **a**–**d**, $I\kappa B\zeta^{+/+}$ (filled symbols/columns) and $I\kappa B\zeta^{-/-}$ (open symbols/columns) peritoneal macrophages were cultured with 10 ng ml^{-1} LPS, 100 ng ml^{-1} BLP, 30 ng ml^{-1} MALP-2, and the indicated concentrations of PGN, R-848 and CpG DNA in the presence of 30 ng ml^{-1} IFN-γ for 24 h. Values are means ± s.d. of triplicate experiments. ND, not detected. **e**, $I\kappa B\zeta^{+/+}$ (filled columns) and $I\kappa B\zeta^{-/-}$ (open columns) MEFs were stimulated with 10 ng ml^{-1} IL-1β and 10 ng ml^{-1} TNF-α. Values are means ± s.d. of triplicate experiments. **f**, Peritoneal macrophages were stimulated with 10 ng ml^{-1} LPS for the indicated periods. Total RNA (5 μg) was extracted and subjected to northern blot analysis for expression of IL-6, TNF-α and β-actin. **g**, Rescue of IL-1 responsiveness in $I\kappa B\zeta^{-/-}$ MEFs by retroviral transfection with full-length (Full), but not deletion mutant (ΔC), IκBζ. Indicated values are means ± s.d. of triplicate experiments. **h**, Double RNA products indicative of IκBζ, IL-6 and TNF-α mRNA transcripts after LPS simulation of wild-type peritoneal macrophages resolved by electrophoresis. Two independent experiments with independently derived wild-type cells were quantified by PhosphoImager (left and middle panels), and mRNA abundance (right panel) is shown for the indicated genes in arbitrary units (left axis, IκBζ and IL-6; right axis, TNF-α) relative to β-actin. Indicated values are means ± s.d. of duplicate experiments.

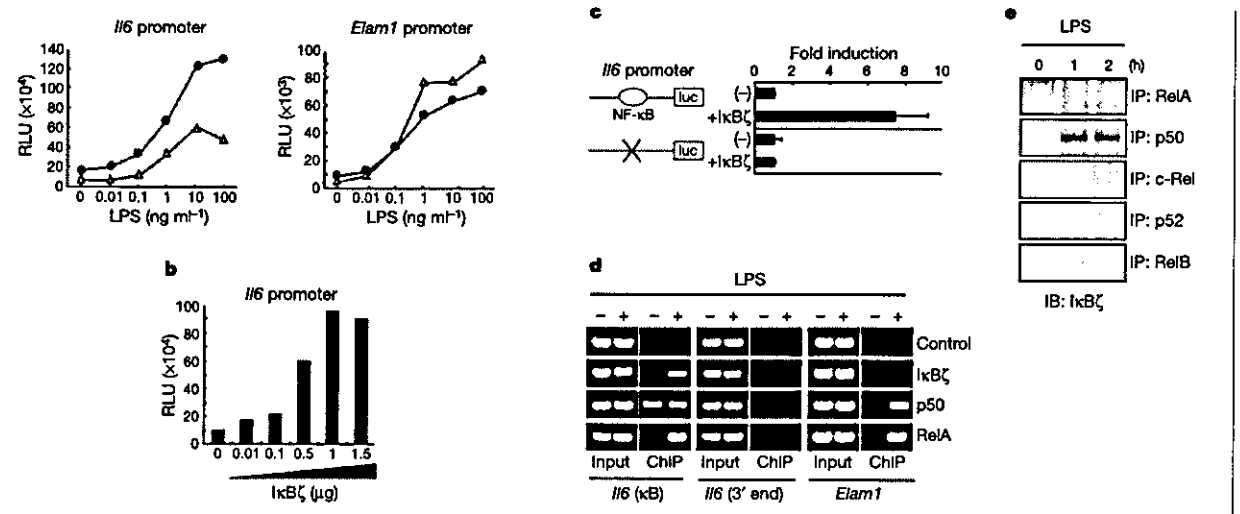

Figure 3 *In vitro* analysis of IκBζ on the *Il6* promoter. **a**, RAW 264.7 cells were transiently transfected with luciferase reporter constructs of either the murine *Il6* promoter or the *Elam1* promoter together with either control (open symbols) or the IκBζ expression plasmid (filled symbols). Luciferase activities are expressed as fold-increase values over the background shown by lysates prepared from untransfected cells. Data are representative of three separate experiments. Cells were stimulated with the indicated concentrations of LPS. RLU, relative luciferase units. **b**, Untreated RAW 264.7 cells were transiently transfected with the IκBζ expression vector together with constant amounts of the *Il6* reporter plasmid. Data are representative of three separate experiments. **c**, P19 cells were transiently transfected with either wild-type or mutant *Il6* promoter reporter constructs together with either control or the IκBζ expression plasmid. Luciferase activities were normalized in each case by dividing the fold-increase values of IκBζ-expressed cells over the background values of lysates with that of mock-expressed cells. Values are means ± s.d. of triplicate experiments. **d**, Chromatin from untreated (−) or LPS-treated (+) (1 μg ml^{-1} for 3 h) RAW 264.7 cells was used for ChIP assays with the indicated antibodies. Precipitated DNA for the *Il6* κB site (left), the 3′ region of the *Il6* gene (centre), or the *Elam1* promoter (right) was assayed by PCR (ChIP). Data are representative of two independent experiments. **e**, Unstimulated or LPS-stimulated (10 ng ml^{-1}) peritoneal macrophages were immunoprecipitated with the indicated antibodies. The immunoprecipitated (IP) lysates were subsequently immunoblotted (IB) with anti-IκBζ.

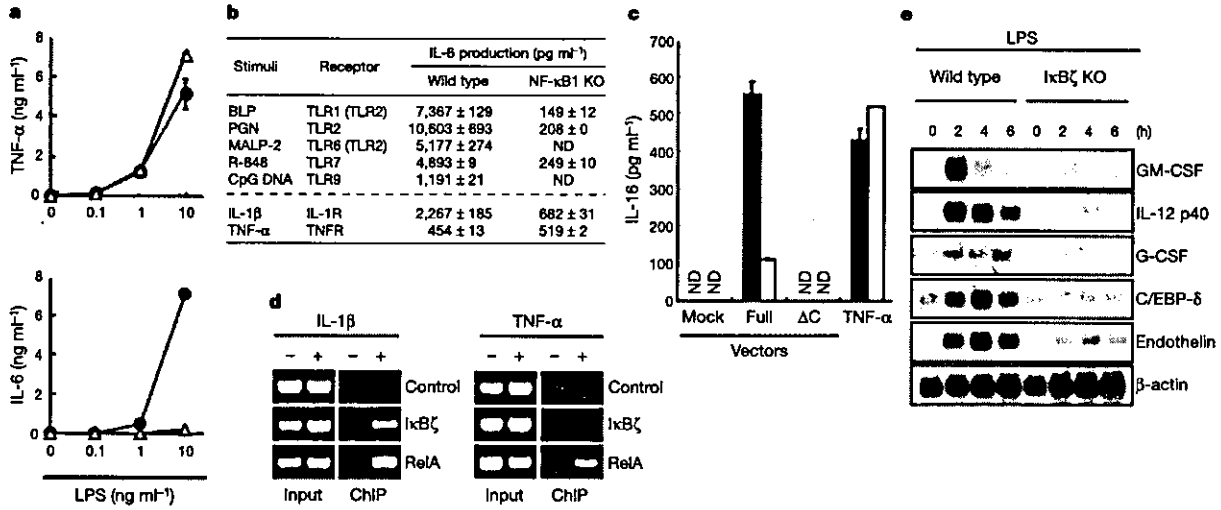

Figure 4 The TLR/IL-1R responses in NF-κB1/p50-deficient cells and microarray analysis of *IκBζ*$^{-/-}$ cells **a**, *NF-κB1*$^{+/+}$ (filled symbols) and *NF-κB1*$^{-/-}$ (open symbols) peritoneal macrophages were cultured with 10 ng ml^{-1} LPS in the presence of 30 ng ml^{-1} IFN-γ for 24 h. Values are means ± s.d. of triplicate experiments. **b**, *NF-κB1*$^{+/+}$ and *NF-κB1*$^{-/-}$ peritoneal macrophages and MEFs were cultured with 100 ng ml^{-1} BLP, 10 μg ml^{-1} PGN, 30 ng ml^{-1} MALP-2, 100 nM R-848, 3 μM CpG DNA, 10 ng ml^{-1} IL-1β or 10 ng ml^{-1} TNF-α in the presence of 30 ng ml^{-1} IFN-γ for 24 h. IL-1β- and TNF-α-induced IL-6 production were analysed by MEFs. Values are means ± s.d. of triplicate experiments. **c**, *NF-κB1*$^{+/+}$ (filled columns) and *NF-κB1*$^{-/-}$ (open columns) MEFs were retrovirally transfected with either the full-length (Full) or the deletion mutant (ΔC) of IκBζ. Furthermore, the same lines of untransfected cells were stimulated with 10 ng ml^{-1} TNF-α. Values are means ± s.d. of duplicate experiments. **d**, Chromatin from untreated (−), IL-1β-treated (left panel (+); 10 ng ml^{-1} for 3 h) or TNF-α-treated (right panel (+); 10 ng ml^{-1} for 3 h) wild-type MEFs were used for ChIP assays with the indicated antibodies. Precipitated DNA for the input (left) or the *Il6* κB site (right) was assayed by PCR. **e**, *IκBζ*$^{+/+}$ and *IκBζ*$^{-/-}$ peritoneal macrophages were stimulated with 10 ng ml^{-1} LPS for the indicated periods. Total RNA (5 μg) was extracted and subjected to northern blot analysis for expression of the indicated probes. GM-CSF, granulocyte-macrophage colony-stimulating factor; G-CSF, granulocyte colony-stimulating factor.